N ~~57~~

58202

NASA CONTRACTOR REPORT 189~~548~~

DELAMINATION ONSET IN POLYMERIC COMPOSITE LAMINATES UNDER THERMAL AND MECHANICAL LOADS

Roderick H. Martin
Analytical Services and Materials, Inc.
Hampton, VA

November 1991

NASA
National Aeronautics and
Space Administration

LANGLEY RESEARCH CENTER
Hampton, Virginia 23665-5225

SUMMARY

This paper describes a fracture mechanics damage methodology to predict edge delamination. The methodology accounts for residual thermal stresses, cyclic thermal stresses and cyclic mechanical stresses. The modelling is based on the classical lamination theory and a sublaminate theory. The prediction methodology determines the strain energy release rate, G, at the edge of a laminate and compares it with the fatigue and fracture toughness of the composite. To verify the methodology, isothermal static tests at 23°C, 125°C, and 175°C and tension-tension fatigue tests at 23°C and 175°C were conducted on laminates. The material system used was a carbon/bismaleimide, IM7/5260. Two quasi-isotropic lay-ups were used, $[45/-45/0/90]_s$ and $[-45/45/90/0]_s$. Also, 24 ply unidirectional double cantilever beam specimens were tested to determine the fatigue and fracture toughness of the composite at different temperatures. Raising the temperature had the effect of increasing the value of G at the edge for these lay-ups and also to lower the fatigue and fracture toughness of the composite. Experimentally, the static stress to edge delamination was not effected by temperature but the number of cycles to edge delamination decreased. The ply interface for delamination was well predicted as was the number of cycles to edge delamination. The static stress predictions tended to overestimate the actual test results, particularly at room temperature.

NOMENCLATURE

A	extensional stiffness matrix
b	specimen width

B	coupling stiffness matrix
D	bending stiffness matrix
E	Young's modulus
f	frequency
G	total strain energy release rate
k	current ply
L	specimen length
M	applied bending moment
ns	number of sublaminates
N	number of plies or load per unit width
P	applied load
$\overline{Q}$	reduced stiffness matrix
R	cyclic load or displacement ratio
t	thickness
T	temperature
u	strain energy density
U	strain energy
V	volume
z	thickness coordinate
α	lamina coefficient of thermal expansion
$\overline{\alpha}$	laminate coefficient of thermal expansion
γ	shear strain
δ	displacement
ΔT	operating temperature - stress free temperature
ϵ	strain
κ	curvature
$\overline{\lambda}$	laminate coefficient of thermal curvature
ν	Poisson's ratio
σ	normal stress
τ	shear stress

Subscripts

1,2,3	fiber, transverse and thickness directions, respectively
ED	referring to edge delamination
i,j	vector directions
I	mode I
II	mode II
Ic	critical mode I value
k	referring to the kth ply
LAM	referring to the laminate properties
min	minimum
max	maximum
s	symmetric
sub	referring to the sublaminate
x,y,z	x,y,z directions

Superscripts

b	bending
c	coupling

e	extensional
M	mechanical
o	mid-surface
T	thermal
*	transposed

INTRODUCTION

With the increased use of laminated fiber reinforced composite materials in primary aircraft structural components, the ability to understand and predict their durability and damage tolerance becomes important. Because of the low transverse strength properties of laminated composites, one of their initial damage modes has been delamination. Delamination is the separation of adjacent plies caused by interlaminar stresses. Although delamination may not result in total collapse of the load bearing properties of the component, it is often a precursor to such an event. An aircraft which experiences high mach numbers as part of its normal flight profile will experience cyclic thermal and mechanical loads. Therefore, a methodology must be established that allows for the prediction of durability and damage tolerance of polymeric composites which experience delamination from these loads.

A life prediction methodology has been established for cyclic mechanical loads at room temperature [1]. This methodology determines the strain energy release rate, G, at possible sources for delamination and compares it to the fatigue and fracture toughness of the composite to predict damage onset. The ability of G to correlate delamination behavior from different sources and to account for different geometric features such as ply thickness and

lay-up is the primary reason for adopting fracture mechanics to analyze delamination problems [1]. In Ref. 2 edge delamination was predicted for a $[45/-45/0/90]_s$, graphite/epoxy laminate using a closed form expression for G. Also in Ref. 2, the accumulation of local delaminations initiating from matrix cracks in the 45° plies in a $[45/-45/0]_s$ laminate was predicted using a different expression for G. The closed form expressions for G in Ref. 2 did not account for the residual thermal stresses and it is these thermal stresses that will vary under elevated temperature or cyclic temperature conditions. Reference 3 described an expression for total G for edge delamination that accounted for the residual thermal and hygroscopic stresses using a sublaminate theory. Similarly, Ref. 4 described an expression for total G for delamination initiating from matrix cracks in off-axis plies, such as 90° or 45° plies. This expression also accounted for residual thermal and hygroscopic stresses.

It is the purpose of this paper to extend the analysis given in Ref. 3 to determine if G can correlate delamination behavior under thermal and mechanical conditions for both static and fatigue loads. First, the modelling is described based on the expressions given in Ref. 3. The analysis of Ref. 3 was extended by allowing the temperature and load to be incremented to represent any type of thermal and mechanical loading. Examples of thermal mechanical loading can include load varying at constant temperature and vice versa, or both temperature and load varying simultaneously. Also, the model was altered to allow for material

property variation of the composite with temperature. For a supersonic aircraft it is anticipated that the aircraft will fly for at least 60,000 hours. It is possible that, during this time, the composite will age and its properties may degrade (or possibly enhance). Also, as the thermal and mechanical loadings continue, damage, such as $90°$ ply cracking, may initiate and accumulate altering the effective material properties. These matrix cracks may be mechanically induced or may occur from thermal aging. Therefore, the modelling allows for material property variation with time due to mechanisms such as lamina stiffness loss due to damage or aging. The matrix cracks may also have an effect on the calculated value of G for edge delamination [5]. However, these effects were not included in the modelling presented here. Although, the effects of moisture absorption on the residual hygroscopic stresses could have been included in the modelling, their effects are not discussed in this paper. The rationale for omitting moisture effects is that all the specimens tested in this work were dried directly before testing and it is unlikely that significant moisture would be absorbed during the elevated temperature tests.

To show how the modelling can be used to predict delamination onset, room and elevated temperature static and tension-tension fatigue tests were conducted on two different quasi-isotropic laminates. The static tests were conducted at room temperature (nominally $23°C$), $125°C$, and $175°C$ and the fatigue tests were conducted at room temperature and $175°C$. While these loadings are

5

generic, they are somewhat analogous to those which a fuselage on an aircraft cruising at a high mach number, or the approach for landing when the aircraft is still hot, may experience. The temperature of 125°C corresponds to approximately mach 2.0 flight and 175°C corresponds to approximately mach 2.4 flight. Also, mode I interlaminar fracture tests were conducted using the double cantilever beam (DCB) specimen. The DCB was tested statically at room temperature, 125°C, and 175°C. The DCB was tested in fatigue at room temperature and 175°C. This interlaminar fracture data was used with the analysis to predict the onset of delamination in the quasi-isotropic laminates.

MATERIALS

The composite material used throughout this study was IM7/5260, a carbon/bismaleimide. Panels for the production of the DCB specimens and the quasi isotropic laminates were produced. The specimen configurations are described in the Test Procedures section. The composite panels were cured in an autoclave according to the following cycle: The temperature was raised from room to 150°C (300°F) at 1.7°C (3°F) per minute under vacuum. The temperature was held at 150°C for 30 minutes and then the pressure was increased to 0.59 MPa (85 psi). The temperature was then raised to 192°C (375°F) at 1.7°C per minute and held for 4 hours. Following the cure, the panels were post cured at room pressure with the following cycle: The temperature was increased from room to 220°C (420°F) at 2.8°C (5°F) per minute and held for 6 hours. The oven was then switched off and the panels allowed to cool in

6

the oven over night (typically 12-15 hours). Following the post cure all the panels were C-scanned to determine panel quality.

The material's elastic constants at various temperatures were determined in Ref. 6 and are repeated here graphically in Fig. 1 with a linear least squares fit to the data. It is these fits that were input into the analysis to determine a particular value of modulus at a particular temperature. The coefficients of thermal expansion and their variation with temperature were determined in this study using a conventional thermal mechanical analysis (TMA) apparatus. Composite samples to measure α_1, α_2, and α_3 were placed in the TMA apparatus. The temperature was raised from room temperature to 550°C at 5°C per minute. The results are shown in Fig. 2. Two specimens were used for each test, one specimen is shown by the circular symbols and the other by square symbols. A linear least squares fit to the data from both specimens is shown and it is these fits that were used in the analysis. The volume fractions for each specimen type are given in the Test Procedures section.

ANALYSIS

Thermal Mechanical G (TMG) Analysis

The strain energy release rate associated with edge delamination may be determined from [3]

$$G = t_{LAM}\, u_{LAM} - \sum_{1}^{ns} t_{sub}\, u_{sub} \qquad (1)$$

where t is the thickness, ns is the number of sublaminates and u is the strain energy density derived from the mechanical, thermal, and

7

moisture loads if considered. The subscript LAM refers to original laminate properties and the subscript sub refers to the properties of the sublaminates formed by edge delamination, Fig. 3. The derivation of the strain energy density in Eq 1 is given in Ref. 3 and is repeated in appendix A.

For cyclic loads and temperatures the strain and the ΔT are constantly changing. Therefore, the strain energy release rate in Eq 1 must be calculated incrementally using the particular strain and temperature at that increment. In addition as the temperature changes the material properties change. Therefore, the material properties corresponding to the current increment of temperature must be used to determine $|\bar{Q}|$, $|A|$, $|B|$, $|D|$, $|\bar{\alpha}|$ and $|\bar{\lambda}|$ for each increment performed. These symbols are defined in the Nomenclature section and used in the appendix. Similarly, if material properties are changing with time, the above matrices must be altered accordingly at each time increment. This analysis will be termed the thermal mechanical G (TMG) analysis throughout the rest of the paper.

Quasi 3 Dimensional Finite Element Analysis

To determine the variation of the individual modes of G as calculated from the TMG analysis, a finite element analysis was used. The analysis was a quasi three dimensional finite element analysis, Q3DG, and was developed in Ref. 7. This analysis was used on the two quasi isotropic laminates studied in the experimental work detailed later. The laminates were subjected to different static loads and temperatures in the analysis. Eight

8

noded quadrilateral, isoparametric elements with three degrees of freedom per node were used to model a cross section in the y-z plane of the specimen. Only one quarter of the cross section was modelled because of symmetry conditions and is shown as the shaded area in Fig. 3. The finite element mesh is shown in Fig. 4. The model consisted of 140 elements having a total of 481 nodes. The smallest element at the delamination front was one eighth of a ply thickness. The delamination front was located approximately seven ply thicknesses from the edge. The analysis was run for temperatures of 23°C, 125°C, and 175°C with the material properties calculated from Figs. 1 and 2. The virtual crack closure technique (VCCT) [7] was used to determine the individual modes and total values of strain energy release rate. However, because the delamination is growing between plies of different orientation the individual modes of G calculated by VCCT will not converge with decreased element size [8]. Therefore, the numerical values of G_I and G_{II} calculated by this method may not be correct. However, the G_I/G ratio was calculated for different applied loads and temperatures using the same element size for all cases and it is the variation of the G_I/G ratio that is used in this paper.

ANALYTICAL RESULTS

Figure 5 shows a typical result from the TMG analysis. The figure represents a fatigue test of a $[45/-45/0/90]_s$ laminate at an isothermal temperature of 175°C (Fig. 5a). The load ratio was R=0.1, the frequency f=5Hz and the strain variation sinusoidal with a maximum strain of 0.004 (Fig. 5b). Figure 5c shows the G

9

variation at the edge in the 0/90 interface, indicated by the arrow in the lay-up definition. The variation of G is no longer a sine wave and has an R-ratio of R=0.01. Figure 6 shows the influence of the change of temperature at different applied strain levels on the value of G at the edge in the 0/90 interface for the same lay-up as above. The temperature is considered to increase from room temperature, nominally 23°C, to the stress free temperature 220°C. At small strain levels, such as those seen during a high cycle (threshold or below) fatigue test, increasing the temperature decreases the value of G at the edge. Therefore, the number of cycles required to cause delamination onset at low strain levels would increase with temperature, assuming that the fatigue interlaminar fracture toughness does not alter with temperature. The influence of temperature on the fatigue and fracture toughness of the composite is discussed in the Experimental Results section. On increasing the strain level to those consistent with static failure or a low cycle fatigue test, an increase in temperature increases the value of G. This result indicates that for this lay-up the laminate will delaminate at lower strains the higher the temperature, again assuming the fatigue interlaminar fracture toughness does not vary with temperature. This phenomena of the effect of temperature on G being dependent on the mechanical strain level arises from the coupling involved in the summation of the product of the strain and stress terms in Eq A4 for the individual plies. Ignoring the bending strains for simplicity, Eq A4 could be expanded to

$$U = \frac{bL}{2} \sum_{k=1}^{N} \int_{z_{k-1}}^{z_k} [\varepsilon_1 \sigma_1 + \varepsilon_2 \sigma_2 + \gamma_{12} \tau_{12}] \, dz \qquad (2)$$

where the strains and stresses are defined by Eqs A6 and A16, respectively. The 1, 2, and 12 terms may be of different sign and may increase in different proportions with a uniform increase in axial strain, thus yielding the result observed in Fig. 6.

Figure 7 shows the effect of material property variation with temperature on G for a $[45/-45/0/90]_s$ and a $[-45/45/90/0]_s$ lay-up. The temperature dependent material properties were taken from Figs 1 and 2 and the temperature independent properties were assumed to be those at room temperature also obtained from Figs. 1 and 2. A constant strain of 0.004 is considered with a temperature increase from room to the stress free temperature. For both lay-ups the change of properties with temperature has a very small effect on the values of G. This suggests that it may be appropriate to determine the linear elastic material properties at room temperature to use in any elevated temperature analysis. However, this may not be true if material non-linearity is considered. Also, it may not be true for all composite material systems and lay-ups.

Figure 8 shows how the TMG analysis may be used as a design tool for determining the best lay-up to use under elevated temperature conditions. Several quasi-isotropic laminates with identical stiffnesses but different ply stacking sequences were analyzed. The laminates were subjected to a strain of 0.004 at a temperature of 175°C. The interface for delamination is indicated

11

by the arrow on the lay-up definition. The figure shows that the values of G vary significantly by altering the lay-up. For laminates with the 90° ply in the interior the values of G are highest indicating the lowest loads required for edge delamination. The laminate with the lowest G is the $[45/90/-45/0]_s$ lay-up.

Figures 9 and 10 show the influence of property degradation with time for a $[45/-45/0/90]_s$ and a $[-45/45/90/0]_s$ lay-up, respectively. The temperature was room temperature with an applied strain of 0.004. Three different situations were studied. The first is an overall degradation of E_{22} to 50 percent of its original value. For the $[45/-45/0/90]_s$ lay-up, this has the effect of very slightly increasing G. Whereas for the $[-45/45/90/0]_s$ lay-up, G is reduced indicating a beneficial effect. The second case is for E_{22} decreasing by 50 percent and G_{12} decreasing by 25 percent. In the first lay-up, G increases with time whereas for the second lay-up, G decreases. The third case studied has E_{22} decreasing by 50 percent, G_{12} decreasing by 25 percent and E_{11} decreasing by 20 percent. Here, for both lay-ups G decreases indicating a beneficial effect. These degradations of properties were arbitrary and severe to show their effect. Matrix cracks, whether thermally aging or mechanically induced, will reduce the individual moduli, however, the magnitude of the reduction may not be as severe as the examples given here.

Figure 11 shows how a simulated flight profile may be characterized using the TMG analysis. The flight profile is fictitious but has a period of constant amplitude sinusoidal

fatigue with rising temperature, indicating take-off and acceleration to cruise. Then a period of cruise where the loads are low and the temperature high. Followed by a period constant amplitude, triangular wave fatigue with slightly decreasing temperature, representing the descent and landing of an hot aircraft.

The TMG analysis and the Q3DG analysis were used to determine the values of G at the edges and the variation of the mode mix, respectively, for the two quasi-isotropic laminates tested in isothermal fatigue, as described in the next section. Figures 12 and 13 show the results using the TMG analysis for a $[45/-45/0/90]_s$ (lay-up A) and a $[-45/45/90/0]_s$ (lay-up B) laminate, respectively. The results are plotted for room temperature, 125°C and 175°C for an increasing strain. For both lay-ups considered in this work, as applied mechanical strain increases the value of G initially decreased and then increased. Also for these lay-ups, the higher the temperature the higher the value of G. Comparing Figs. 12 and 13 at the same strain and temperature, the value of G for lay-up A is higher than for lay-up B, indicating that lay-up A will delaminate at lower loads than lay-up B.

Figure 14 shows a plot of the G_I/G ratio versus the applied strain at 23°C, 125°C, and 175°C. The previous note on the accuracy of the numerical values of the individual modes of G is reiterated, however, the results are only used in a qualitative manner and hence are satisfactory. For both lay-ups, as the applied load increases, the percentage of mode I increases. Also, as

13

temperature increases the mode I percentage increases. However, at the higher temperatures the mode I percentage plateaus at a much lower strain than at room temperature.

TEST PROCEDURES

The following section describes the experimental work conducted. Two different quasi-isotropic laminates and DCB specimens were tested statically and in fatigue at room and elevated temperatures. Prior to testing, all specimens were dried using the following cycle: 1 hour at 95°C, 1 hour at 110°C, 16 hours at 125°C and 1 hour at 150°C. Following the drying cycle, the specimens were stored in a desiccator cabinet for no longer than seven days prior to testing.

Quasi-isotropic Laminate Static and Fatigue Testing

The specimens for the experimental study consisted of two different, 8-ply, symmetric, quasi-isotropic laminates, $[45/-45/0/90]_s$, lay-up A and $[-45/45/90/0]_s$, lay-up B. Each specimen measured 250x25mm with the 0° degree fibers being in the longest length direction. The specimens had a nominal thickness of 1.2mm. The edges of the specimens were painted with a white, water soluble, typewriter correction fluid to aid the observation of delamination onset. The specimens had an average volume fraction of 54.6 percent.

The static tests on the quasi isotropic laminates were conducted under displacement control at a loading rate of 0.5 mm/min at room temperature, 125°C, and 175°C. At least four specimens were used per temperature. The fatigue tests were all

conducted under load control at a frequency of 5Hz and at an R-ratio (P_{min}/P_{max}) of R=0.1 at room temperature and 175°C. For the elevated temperature tests, quartz lamps were placed either side of the specimen. The overall temperature variation throughout the test was ±2°C. The test temperature along the length varied by ±2°C. One thermocouple was used to control the test temperature and was placed in the center of the gauge area. The specimens were gripped in the top and bottom jaws and the temperature increased to the desired value. The set-up was then left for five minutes to reach thermal equilibrium. The initial load or strain was zeroed and the test begun. Displacement transducers (DCDT) were used to determine strains. The gauge length varied from specimen to specimen but was typically between 50 and 75mm. For the static tests the loads and displacements were stored digitally and on an X-Y recorder. An X-Y recorder was used to allow the load at which delamination onset at the edge became visible to be noted on the chart. When delamination was visually observed on the edges an X-ray was taken to confirm that delamination had (or had not) occurred. A zinc iodide dye penetrant was used. Periodically throughout the fatigue tests, the tests were stopped and the specimen unloaded. Laminate stiffness was then determined by loading the laminate up to the mean load and then the fatigue test was resumed. During this procedure, for the room temperature tests only, an X-ray was taken of the laminate at mean load to determine the extent of damage. No X-rays were taken during the elevated temperature tests because a suitable dye penetrant that would not

burn off at the elevated temperature and was also non-toxic was not found. However, X-rays were taken after the tests were completed and damage had been observed visually.

Double Cantilever Beam Tests

Double cantilever beam specimens were fabricated to determine the mode I fatigue and static fracture toughness of the composite. The specimens were 24-ply, 0° unidirectional laminates. A 13μm non-adhesive Teflon film was placed at the mid-plane at one end prior to curing to simulate a delamination. The specimen dimensions were 100 X 25mm. The specimens had a volume fraction of 58.9 percent. Piano hinges were bonded to the surface to allow load to be transferred to the beam.

The static tests were conducted under displacement control at a loading rate of 0.5 mm/min at room temperature, 125°C, and 175°C. Four specimens per temperature were tested. Interlaminar fracture toughness, G_{Ic}, was determined for a delamination initiating from the end of the thin insert [9]. Initiation of delamination corresponded to the deviation from linearity of the load-displacement plot. This deviation from linearity occurred at the same loads and displacements that the delamination was visually seen to grow at the edge. Using the procedure given in Ref. 10, the fatigue tests were conducted under displacement control at an R-ratio ($\delta_{min}/\delta_{max}$) of R=0.1, at a frequency of 5Hz at various maximum cyclic displacements at room temperature and at 175°C. The number of cycles to delamination onset was determined by monitoring the maximum cyclic load, P_{max}. If a 1 percent decrease in P_{max} was

16

observed then the delamination was assumed to have grown. Delamination growth was always confirmed visually. All the elevated temperature tests were conducted using quartz lamps as the heating source.

EXPERIMENTAL RESULTS

Figure 15 shows the loss in stiffness with fatigue cycles for a typical specimen of lay-up A at room temperature. The loss in stiffness is small, approximately 1 percent per 100,000 cycles for a specimen tested at a maximum cyclic stress of 309 N/mm^2. This minor loss in stiffness is caused by cracking in the 90° plies prior to edge delamination. Figure 16 shows an X-radiograph of a typical specimen of lay-up A after a static test. The matrix cracks in the 90° plies are clearly visible as is the edge delamination. No cracks in the 45° plies are visible. Also shown in Fig. 16 is a micrograph of the polished edge of lay-up A. The matrix cracks in the 90° plies and the delamination are again clearly visible. There is no evidence of an interfacial failure between the fiber and the matrix. Lay-up B experienced similar damage with matrix cracks forming in the 90° plies followed by both 0/90 interfaces delaminating.

Figure 17 shows the results of the static tests for lay-ups A, open square symbols, and B, open circular symbols, at the three different temperatures, where σ_{ED} is the applied stress that produced the edge delamination. The lines are predictions and will be discussed in the next section. For all three temperatures, lay-up B required a larger stress before edge delamination than

17

lay-up A as indicated by the lower G for that lay-up in Figs. 12 and 13. For both lay-ups increasing the temperature had little effect on the stress for edge delamination. This is in contrast to Figs. 12 and 13 which indicated a higher G and hence a lower stress. However, the scatter of the results seems larger at the higher temperatures and the true trend in the stress at edge delamination may be masked by this scatter. The reason for the increase in scatter is not known. Also, the effect of the matrix cracks on the delamination was not included in the modelling and may effect the calculated values of G.

Figures 18 and 19 show the fatigue results for both lay-up A and B at room temperature and 175°C, respectively. Lay-up A is plotted as open square symbols and lay-up B as open circular symbols. The results are plotted as the maximum applied cyclic stress versus the number of cycles to delamination onset. Also plotted are the static stresses to delamination onset from Fig. 17 for comparison. Similarly to the static results, lay-up B required more cycles at both temperatures before the onset of delamination because of the lower value of G at the edge as indicated in Figs. 12 and 13. Figures 20 and 21 show the effect of temperature on the number of cycles to delamination for lay-ups A and B, respectively. For both laminates increasing the temperature decreased the required number of cycles to edge delamination onset as indicated by the higher values of G at the higher temperatures in Figs. 12 and 13 and by the decrease in the fatigue toughness of the composite as detailed next. Also, for both lay-ups the room

temperature curves are flatter than the elevated temperature ones.

Figure 22 shows the results of the DCB static and fatigue tests at room temperature and elevated temperatures. Raising the test temperature decreased the static interlaminar fracture toughness by a small amount. The DCBs tested at 175°C showed marked permanent deformation following testing whereas those tested at 23°C and 125°C did not. This permanent deformation had seemingly no effect on the initiation values of interlaminar fracture toughness but produced a more marked R-curve effect, not shown. Unlike the static results, raising the temperature had a big effect on the fatigue interlaminar fracture toughness, decreasing it significantly. This indicates that fatigue may be an issue for the damage tolerance of an hot structure.

PREDICTIONS AND DISCUSSION

Using the TMG analysis and the results from the DCB static and fatigue tests it is possible to predict the number of cycles and the stress to delamination of the two quasi-isotropic laminates. To predict the static stress to delamination onset the highest and lowest (scatter) values of the interlaminar fracture toughness, G_{Ic}, results from the DCB specimens at each temperature were used with Figs. 12 and 13 to determine the corresponding strain to yield those values of G_{Ic}, these were the predicted strains. Even though there was extensive ply-cracking in the 90° plies, there was little decrease in stiffness prior to delamination. Hence, the calculated modulus at the specific temperature, prior to damage, was used to determine the predicted static stress to delamination onset from

the strain values. The range of predicted stress to edge delamination is shown in Fig. 17 for lay-ups A and B. For lay-up A the predictions were consistently higher than the experimental results, except the 175°C tests. The scatter is low in the DCB tests and hence the range of the predictions was low. For the lay-up B room temperature tests the predictions are also somewhat unconservative. However, for the elevated temperature tests the predictions are within experimental data scatter. Again the range of the predictions is smaller than the scatter of the experiments.

To predict the number of cycles to delamination onset the same method was used. However, no scatter curves or statistical fits were made to the DCB fatigue data. Instead each individual fatigue result was used by using the value of G_{Imax} and its relative number of cycles to delamination onset with Figs. 12 or 13 and assuming that the G in those figures is now G_{max}. Hence, a value of ϵ_{max} can be determined at the specific number of cycles [11]. Again the stiffness loss was considered small and the original laminate modulus was used to calculate σ_{max} at the specific number of cycles. The results of this procedure are shown in Figs. 23-26. Figure 23 shows the predictions for lay-up A at room temperature. Contrary to the static predictions, also shown on Fig. 23, the fatigue predictions are well within the experimental scatter. Figure 24 shows a similar plot for lay-up B at room temperature. Here the predictions are close at the low cycle end but are conservative at the high cycle end. Figure 25 shows the predictions for lay-up A at 175°C. In this case both the static and the fatigue results are

predicted very well. Figure 26 shows the results for lay-up B at 175°C, again both the static and fatigue results are predicted well.

One possible reason for the prediction of the room temperature fatigue tests of lay-up B being conservative at the high cycle end, Fig. 24, is that a total G is being calculated and compared with a mode I fatigue toughness. As the applied cyclic strain/stress decreases the quantity of G_{II} increases, Fig. 14. Increasing the mode II component increases the static toughness [12] and it is probable that the same effect would happen in fatigue, although this still needs to be verified. The room temperature predictions of lay-up A show only a very slight conservative trend at the high cycle fatigue end, Fig. 23. Although the mode II component does increase at lower cyclic strains/stresses, it is less severe than lay-up B. The predictions of lay-ups A and B at 175°C, Figs. 25 and 26, showed less conservatism at the high cycle end than the room temperature predictions because the mode I component is constant over much of the applied cyclic strain/stress range, Fig. 14.

This work has shown how delamination onset predictions may be made by calculating a total G and comparing it to the mode I interlaminar fracture toughness. However, if there is significant mode II component the prediction will be conservative. The accuracy of these predictions is a step toward predicting the damage tolerance of composite structures experiencing thermal and mechanical loads. By analyzing structures for possible sources of

delamination and determining a value of G it is possible to predict delamination onset using DCB data tested under the same environmental conditions. However, several effects may need to be included to predict the real time damage tolerance of a supersonic transport aircraft. The effects of materials aging have already been mentioned and may be included by altering the material properties with time, if known. The effect of aging on the static and fatigue fracture toughness would also have to be taken into consideration. The effect of matrix cracking from mechanical loads or thermal aging have not been accounted for. It is likely that they may have a large effect on the values of G. Reference 4 detailed an expression for G for local delaminations emanating from matrix cracks. The TMG analysis could be run using this expression for G and assuming that the edge delamination is a series of local delaminations originating from the matrix crack and linking with each other. Also, the TMG analysis considered the material to be linear elastic. For some materials this assumption may be inaccurate at the higher temperatures. Also, some of the sublaminates that may form on delamination will have no zero degree fibers, as in laminate B and may behave nonlinearly especially at elevated temperature. To account for these material nonlinearities a viscoplastic methodology described in Ref. 13 would be required. Similarly, the TMG analysis does not account for viscoelastic effects. For a supersonic transport aircraft much of its flight time will spent at high mach cruise. It is in this profile that creep and relaxation effects will be largest.

SUMMARY

This paper described a fracture mechanics damage methodology to predict edge delamination. The methodology accounts for residual thermal stresses, cyclic thermal stresses and cyclic mechanical stress. The modelling was based on the classical lamination theory and a sublaminate theory. The prediction methodology determines the strain energy release rate, G, at the edge of a laminate and compares it with the fatigue and fracture toughness of the composite. To verify the methodology, isothermal static tests at room temperature 23°C, 125°C, and 175°C and tension-tension fatigue tests at 23°C and 175°C were conducted on laminates. The material system used was a carbon/bismaleimide, IM7/5260. Two quasi-isotropic lay-ups were used, (45/-45/0/90)$_s$ and (-45/45/90/0)$_s$. Also, 24 ply, unidirectional double cantilever beam specimens were tested to determine the fatigue and fracture toughness of the composite at different temperatures. Raising the temperature had the effect of increasing the value of G for these lay-ups and also to lower the fatigue and fracture toughness of the composite. Experimentally, the static stress to edge delamination was not effected by temperature but the number of cycles to edge delamination decreased. The ply interface for delamination was well predicted as was the static strain and the number of cycles to edge delamination. The static stress predictions tended to overestimate the actual test results, particularly at room temperature.

REFERENCES

1. O'Brien, T.K., "Towards a Damage Tolerance Philosophy for Composite Materials and Structures," <u>Composite Materials: Testing and Design</u> (Ninth Volume), ASTM STP 1059, S.P. Garbo, Ed., 1990, pp. 7-33.

2. O'Brien, T.K., Rigamonti, M., and Zanotti, C., "Tension Fatigue Analysis and Life Prediction for Composite Laminates," Int. J. Fatigue, 11, No. 6, November 1989, pp. 379-393.

3. O'Brien, T.K., Raju, I.S., and Garber, D.P., "Residual Thermal and Moisture Influences on the Strain Energy Release Rate Analysis of Edge Delamination," Journal of Composites Technology and Research, Vol. 8. No.2, Summer 1986, pp. 37-47.

4. O'Brien, T.K., "Residual Thermal and Moisture Influences on the Strain Energy Release Rate Analysis of Local Delaminations From Matrix Cracks," to be published in Journal of Composites Technology and Research. Also published as NASA TM 104077, Hampton, Virginia, 1991.

5. Salpekar, S.A. and O'Brien, T.K., "Combined Effect of Matrix Cracking and Free Edge on Delamination," <u>Composite Materials: Fatigue and Fracture (Third Volume)</u>, ASTM STP 1110, T.K. O'Brien, Ed., American Society for Testing and Materials, Philadelphia, 1991, pp. 287-311.

6. Gates, T.S., "Experimental Characterization of Nonlinear, Rate Dependent Behavior in Advanced Polymer Matrix Composites," proceedings of the 1991 SEM Spring Conference on Experimental Mechanics, June 9-12, 1991, Milwaukee, Wisconsin, pp. 639-646.

7. Raju, I.S., "Q3DG - A Computer Program for Strain-Energy-Release Rates for Delamination Growth in Composite Laminates," NASA CR 178205, Hampton, Virginia, November 1986.

8. Sun, C.T. and Jih, C.J., "On the Strain Energy Release Rates for Interfacial Cracks in Bi-Material Media," Engineering Fracture Mechanics, 28:13-27, 1987.

9. Murri, G.B. and Martin R.H., "Effect of Initial Delamination on Mode I and Mode II Interlaminar Fracture Toughness and Fatigue Fracture Threshold," presented at the 4th ASTM Symposium on Composite Materials: Fatigue and Fracture, Indianapolis, Indiana, May 6-9, 1991. Also published as NASA TM 104079, Hampton, Virginia, May 1991.

10. Martin, R.H., "Characterizing Mode I Fatigue Delamination of Composite Materials," Proceedings of the Mechanics Computing in 1990's and Beyond Conference, Columbus, Ohio, May 19-22, 1991, Vol. 2, pp. 943-948.

11. Murri, G.B., Salpekar, S.A., and O'Brien, T.K., "Fatigue Delamination Onset Prediction in Tapered Composite Laminates," <u>Composite Materials: Fatigue and Fracture (Third Volume)</u>, ASTM STP 1110, T.K. O'Brien, Ed., American Society for Testing and Materials, Philadelphia, 1991, pp. 312-339.

12. Reeder, J.R. and Crews, J.H., Jr., "Re-Design of the Mixed Mode Bending Test for Delamination Toughness," proceedings of ICCM VIII, Composites, Design and Manufacture, Eds. Tsai, S.W. and Springer, G.S., SAMPE, Covina, July 1991, 36-B.

13. Gates, T.S., "Effects of Elevated Temperature on the Viscoplastic Behavior of Advanced Polymer Matrix Composites," presented at the ASTM Symposium on High Temperature and Environmental Effects on Polymeric Composites, San Diego, California, October 15th, 1991.

14. Jones, R.M. "Mechanics of Composite Materials," McGraw-Hill Book Company, New York, 1975.

APPENDIX A

The strain energy release rate associated with edge delamination may be determined from [3]

$$G = t_{LAM} \, u_{LAM} - \sum_{1}^{ns} t_{sub} \, u_{sub} \qquad (A1)$$

where t is the thickness, ns is the number of sublaminates and u is the strain energy density derived from the mechanical, thermal, and moisture loads if considered. For a laminate consisting of N plies of various thicknesses the strain energy density may be determined from the strain energy, U, thus

$$u = \frac{U}{bLt} \qquad (A2)$$

where b is the laminate width and L is the laminate length. The strain energy of a given volume, V, may be expressed in terms of the stress and strain tensors thus

$$U = \frac{1}{2} \int_V \varepsilon_{ij} \, \sigma_{ij} \, dV \qquad (A3)$$

If the volume is composed of orthotropic laminae and a state of plane stress is assumed, the strain energy may be redefined in terms of individual lamina stress and strain. Thus,

$$U = \frac{bL}{2} \sum_{k=1}^{N} \int_{z_{k-1}}^{z_k} |\varepsilon|_k^* \, |\sigma|_k \, dz \qquad (A4)$$

where the bars, $|x|$, indicate a matrix, z is the z-coordinate dimension, and the superscript * indicates the matrix is transposed. The total strain in any ply is given by the sum of the

midplane strain, $|\epsilon^o|$, and the product of the curvature $|\kappa|$ and the distance from the mid-plane, z, thus

$$|\epsilon| = |\epsilon^o| + z \, |\kappa| \tag{A5}$$

The curvatures will only be present in unsymmetric laminates or sublaminates and when the laminate is subjected to bending. When the laminates or sublaminates are unsymmetric, the resulting curvatures will create bending and bending-extensional coupling terms of the strain energy density as described below. The mid-plane strains and curvatures will be composed of the applied mechanical strain, indicated by a superscript M, and the applied thermal strain, indicated by a superscript T, thus

$$|\epsilon| = |\epsilon^o|^M + |\epsilon^o|^T + z \, \{ \, |\kappa|^M + |\kappa|^T \, \} \tag{A6}$$

For the applied mechanical strain vector, $|\epsilon^o|^M$, the restraints imposed by the gripping conditions of the testing machine for a flat laminate must be considered. The axial strain, ϵ_x, is the known applied strain and the grips of the test machine impose the following boundary conditions away from the grips [3,4]

$$N_y = \gamma_{xy} = \kappa_x = M_y = \kappa_{xy} = 0 \tag{A7}$$

thus the mechanical strain vector can be determined from

$$
\begin{vmatrix} \epsilon_x^o \\ \epsilon_y^o \\ 0 \\ 0 \\ \kappa_y \\ 0 \end{vmatrix}^M = \begin{vmatrix} A & B \\ B & D \end{vmatrix}^{-1} \begin{vmatrix} N_x \\ 0 \\ N_{xy} \\ M_x \\ 0 \\ M_{xy} \end{vmatrix}
\tag{A8}
$$

where A, B, and D are the stiffness matrices defined in Ref. 14. The ply strains may be determined from [3]

$$|\varepsilon|_k = |\varepsilon^o|^M + (|\bar{\alpha}| - |\alpha|_k) \Delta T + z \{ |\kappa|^M + |\bar{\lambda}| \Delta T \} \qquad (A9)$$

$$= |R|_k + z |S|_k \qquad (A10)$$

where

$$|R|_k = |\varepsilon^o|^M + (|\bar{\alpha}| - |\alpha|_k) \Delta T \qquad (A11)$$

$$|S|_k = |\kappa|^M + |\bar{\lambda}| \Delta T \qquad (A12)$$

ΔT is the difference between the operating temperature and the stress free temperature thus

$$\Delta T = T_{operating} - T_{stress\ free} \qquad (A13)$$

$|\alpha|_k$ is the thermal coefficient vector for each ply, $|\bar{\alpha}|$ and $|\bar{\lambda}|$ are the laminate coefficients of expansion and curvature, respectively, and are defined as [14]

$$\begin{vmatrix} \bar{\alpha} \\ \bar{\lambda} \end{vmatrix} = \frac{1}{\Delta T} \begin{vmatrix} A & B \\ B & D \end{vmatrix}^{-1} \begin{vmatrix} N \\ M \end{vmatrix}^T = \frac{1}{\Delta T} \begin{vmatrix} A & B \\ B & D \end{vmatrix}^{-1} \sum_{k=1}^{N} |\bar{Q}|_k \begin{vmatrix} |\alpha|_k\ t_k \\ |\alpha|_k\ \frac{1}{2}(z_k^2 - z_{k-1}^2) \end{vmatrix} \qquad A14$$

where $|\bar{Q}|_k$ is the transformed reduced stiffness matrix [14]. For the sublaminates formed by edge delamination in Eq 1 the thermal expansion in the x-direction is assumed to be equal to the thermal expansion of the laminate [3]. Therefore for the sublaminates

$$| \overline{\alpha} | = \begin{vmatrix} \overline{\alpha}_{x_{LAM}} \\ \overline{\alpha}_{y_{sub}} \\ \overline{\alpha}_{xy_{sub}} \end{vmatrix} \qquad (A15)$$

The $|\sigma|_k$ vector in Eq A4 is given by the product of the transformed reduced stiffness matrix $|\widetilde{Q}|_k$ and the strain thus

$$|\sigma|_k = |\overline{Q}|_k \, |\varepsilon|_k = |\overline{Q}|_k \, \{|R|_k + z \, |S|_k\} \qquad (A16)$$

Substituting Eqs A10 and A16 into Eq A4 the strain energy may be re-written as

$$U = \frac{bL}{2} \sum_{k=1}^{N} \int_{z_{k-1}}^{z_k} \{|R|_k + z \, |S|_k\}^* \, |\overline{Q}|_k \, \{|R|_k + z \, |S|_k\} \, dz \qquad (A17)$$

Integrating Eq A17 between the limits and factoring out $(z_k - z_{k-1}) = t_k$ the strain energy may be written as

$$U = \frac{bL}{2} \sum_{k=1}^{N} t_k \, \{ \, |R|_k^* \, |\overline{Q}|_k \, |R|_k + \frac{1}{3} \, (z_k^2 + z_k z_{k-1} + z_{k-1}^2) \, |S|_k^* \, |\overline{Q}|_k |S|_k +$$

$$(z_k + z_{k-1}) \, |R|_k^* \, |\overline{Q}|_k \, |S|_k \, \} \qquad (A18)$$

$$= b \, L \sum_{k=1}^{N} u_k \, t_k \qquad (A19)$$

Therefore, u_k is the strain energy density for each ply and is a summation of the extensional, u_k^e, the bending, u_k^b and the bending extension coupling, u_k^c, strain energy density for each ply thus

$$u_k = u_k^e + u_k^b + u_k^c \qquad (A20)$$

Expressing terms R and S in full from Eq A18 and assuming all plies have equal thickness

$$u_k^e = \frac{1}{2N} \left[\ |\varepsilon^o|^M + (|\overline{\alpha}| - |\alpha|_k) \Delta T \ \right]^* |\overline{Q}|_k \left[\ |\varepsilon^o|^M + (|\overline{\alpha}| - |\alpha|_k) \Delta T \ \right] \quad \text{(A21)}$$

$$u_k^b = \frac{1}{6N} \{ z_k^2 + z_k z_{k-1} + z_{k-1}^2 \} \left[\ |\kappa|^M + |\overline{\lambda}| \Delta T \ \right]^* |\overline{Q}|_k \left[\ |\kappa|^M + |\overline{\lambda}| \Delta T \ \right]$$

$$\text{(A22)}$$

$$u_k^c = \frac{1}{2N} \{ z_k + z_{k-1} \} \left[\ |\kappa|^M + |\overline{\lambda}| \ \Delta T \ \right]^* |\overline{Q}|_k \left[\ |\varepsilon^o|^M + (|\overline{\alpha}| - |\alpha|_k) \ \Delta T \ \right]$$

$$\text{(A23)}$$

For symmetric laminates and sublaminates Eqs A22 and A23 are zero and only the extensional strain energy density contributes to the strain energy release rate in Eq 1.
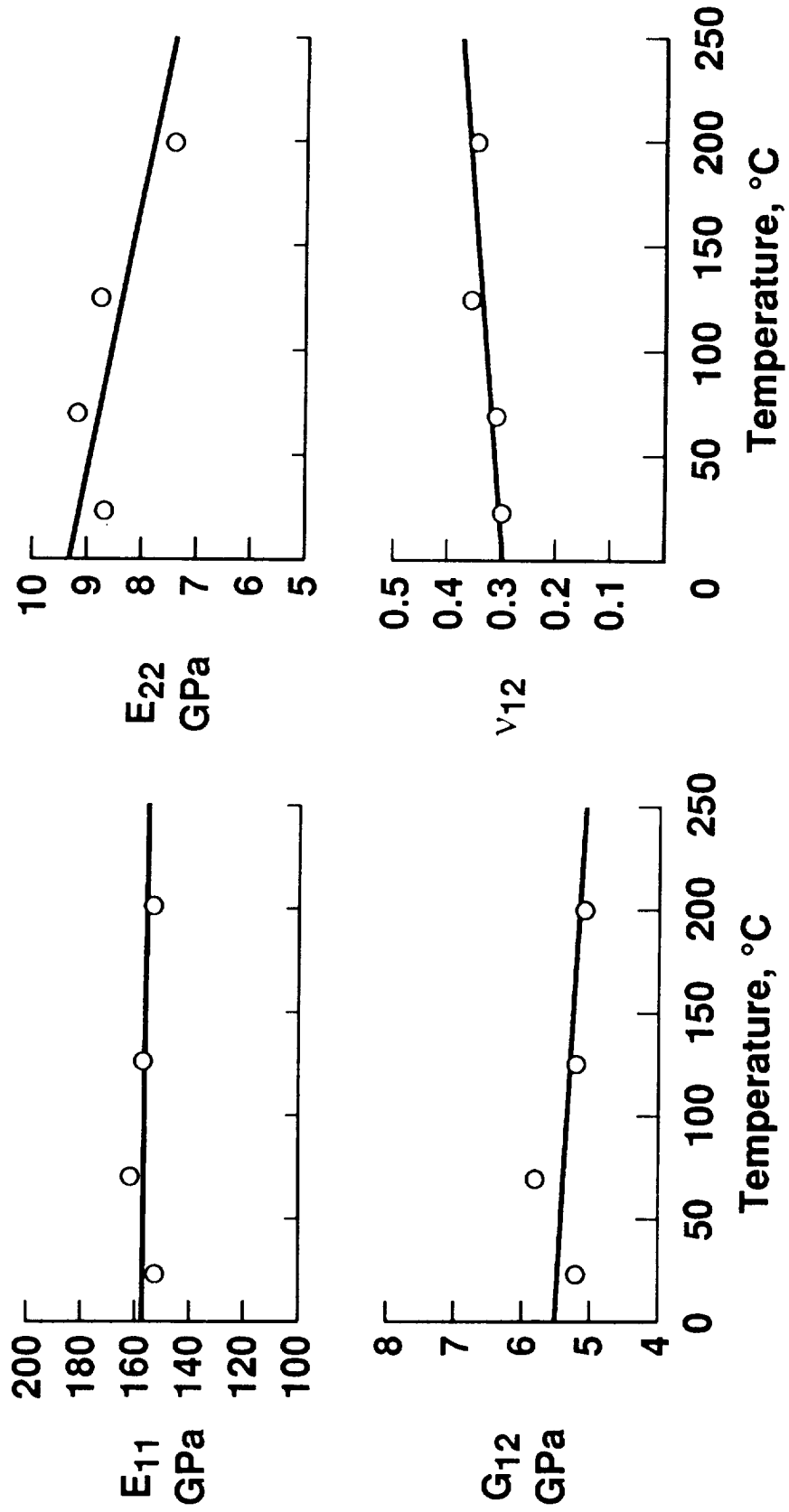
Fig. 1   Moduli versus temperature for IM7/5260 [6].
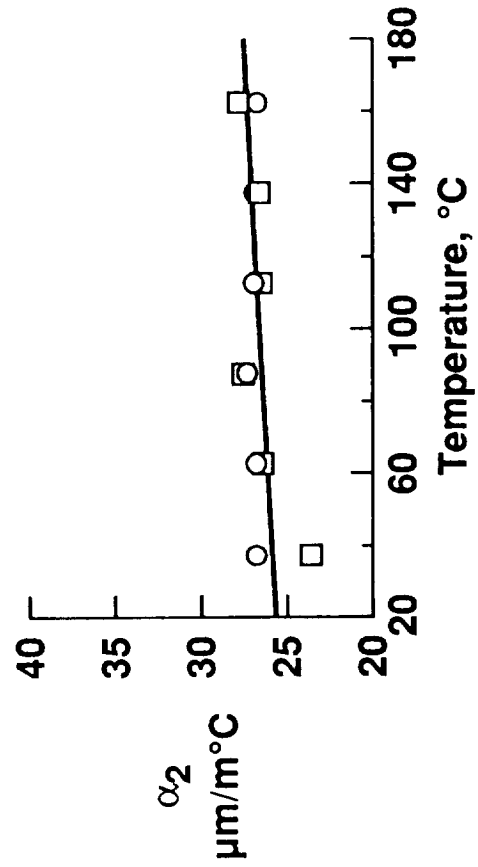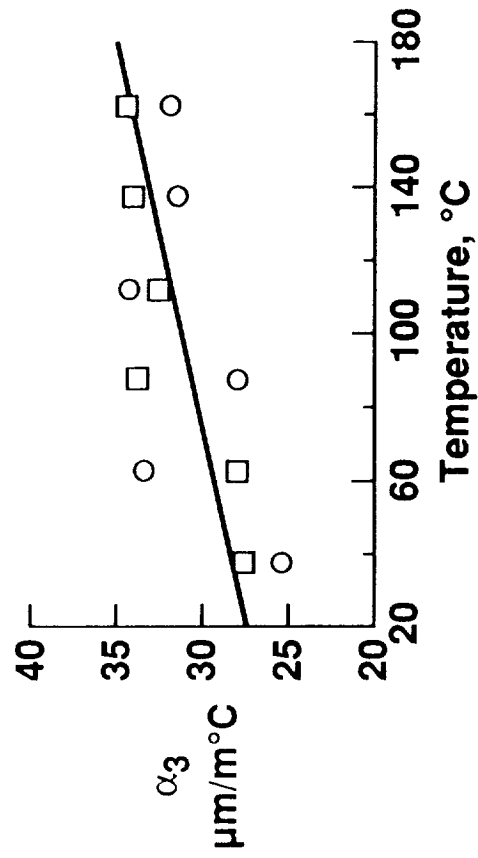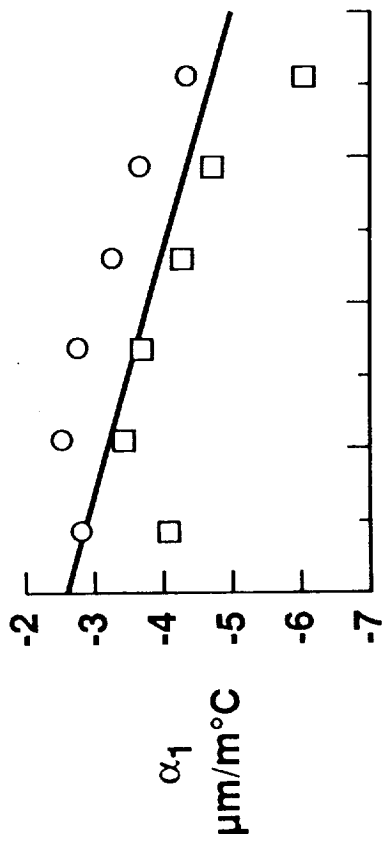
Fig. 2   Coefficients of thermal expansion versus temperature for
IM7/5260.

32
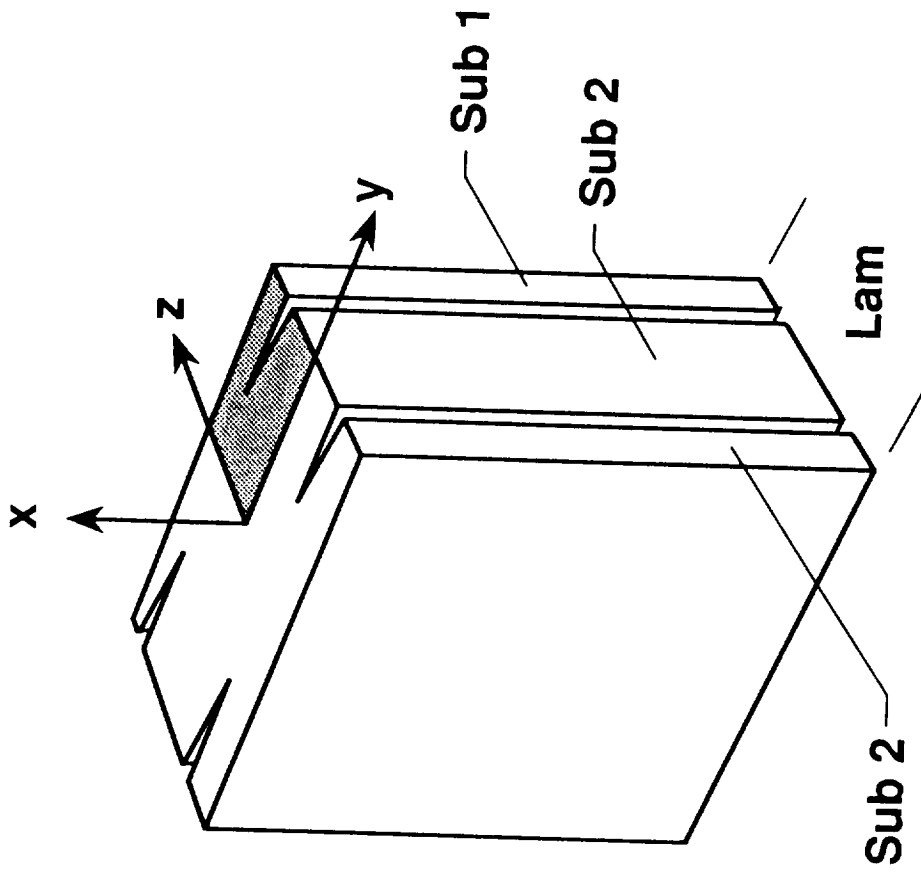
Fig. 3   Schematic of edge delamination.

y and z dimensions on different scales
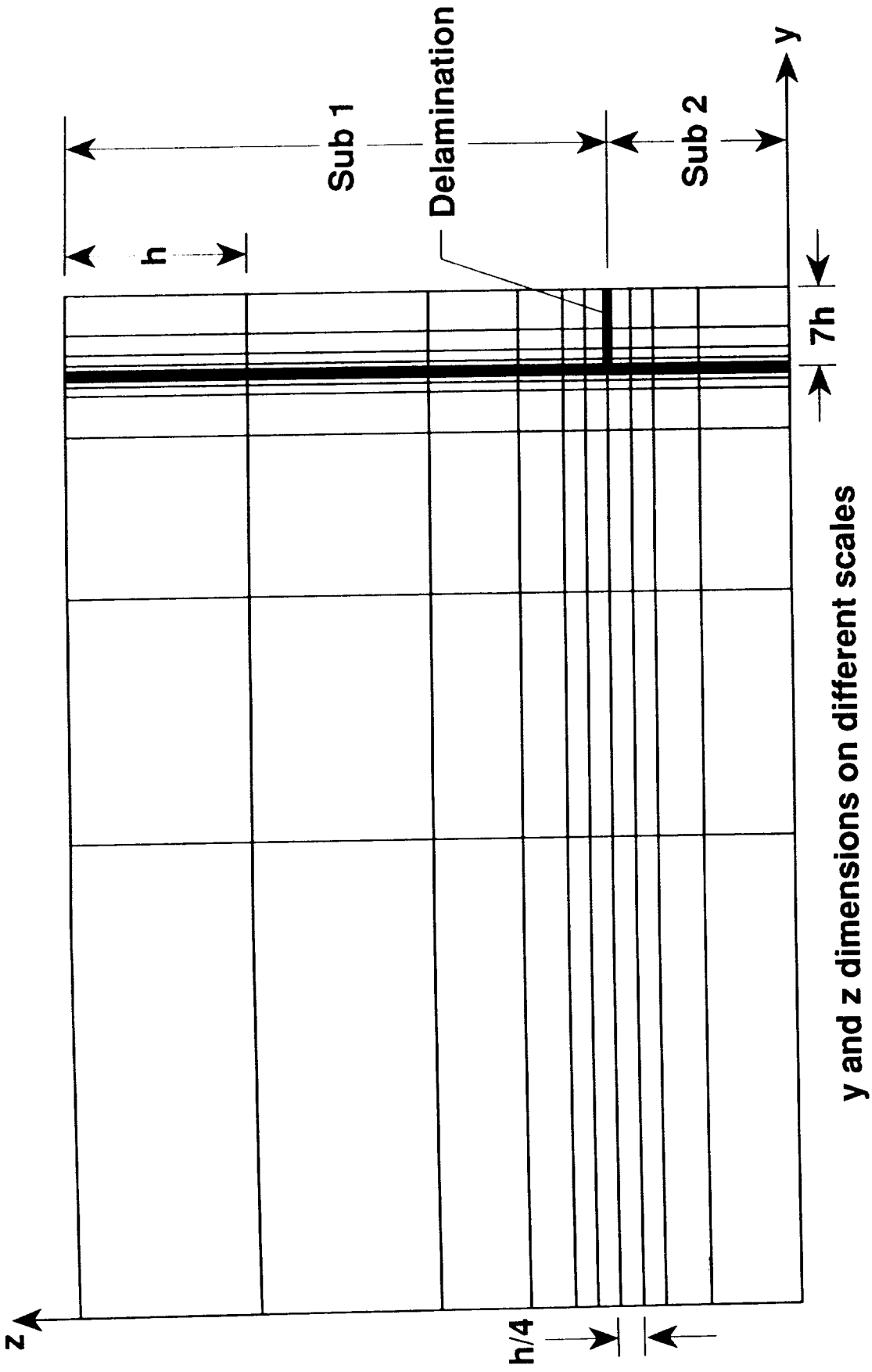
Fig. 4   Finite element mesh for quasi-three dimensional analysis.
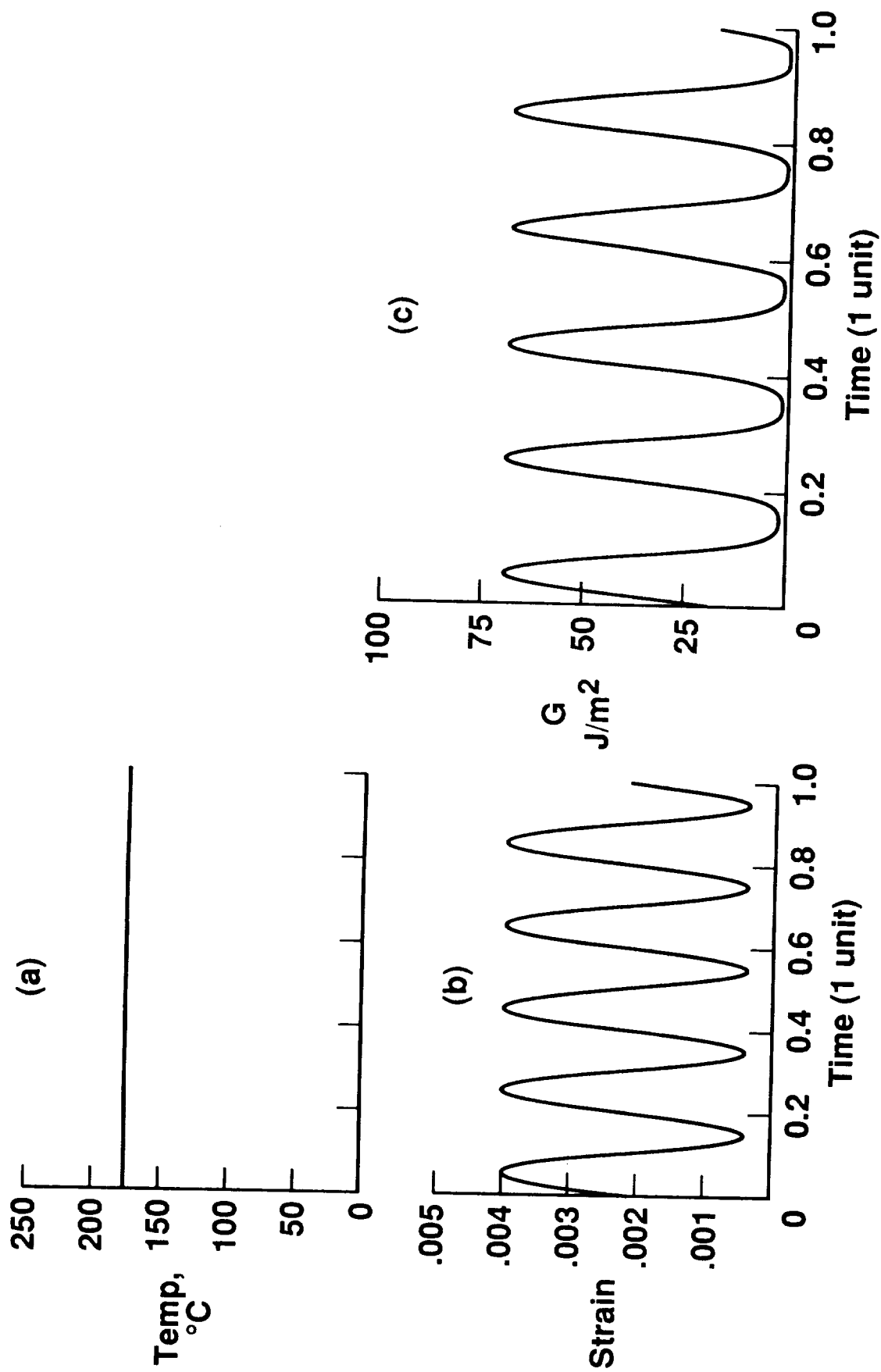
Fig. 5   G values at the edge of a [45/-45/0/90]$_s$ laminate under sinusoidal mechanical fatigue at 175°C.
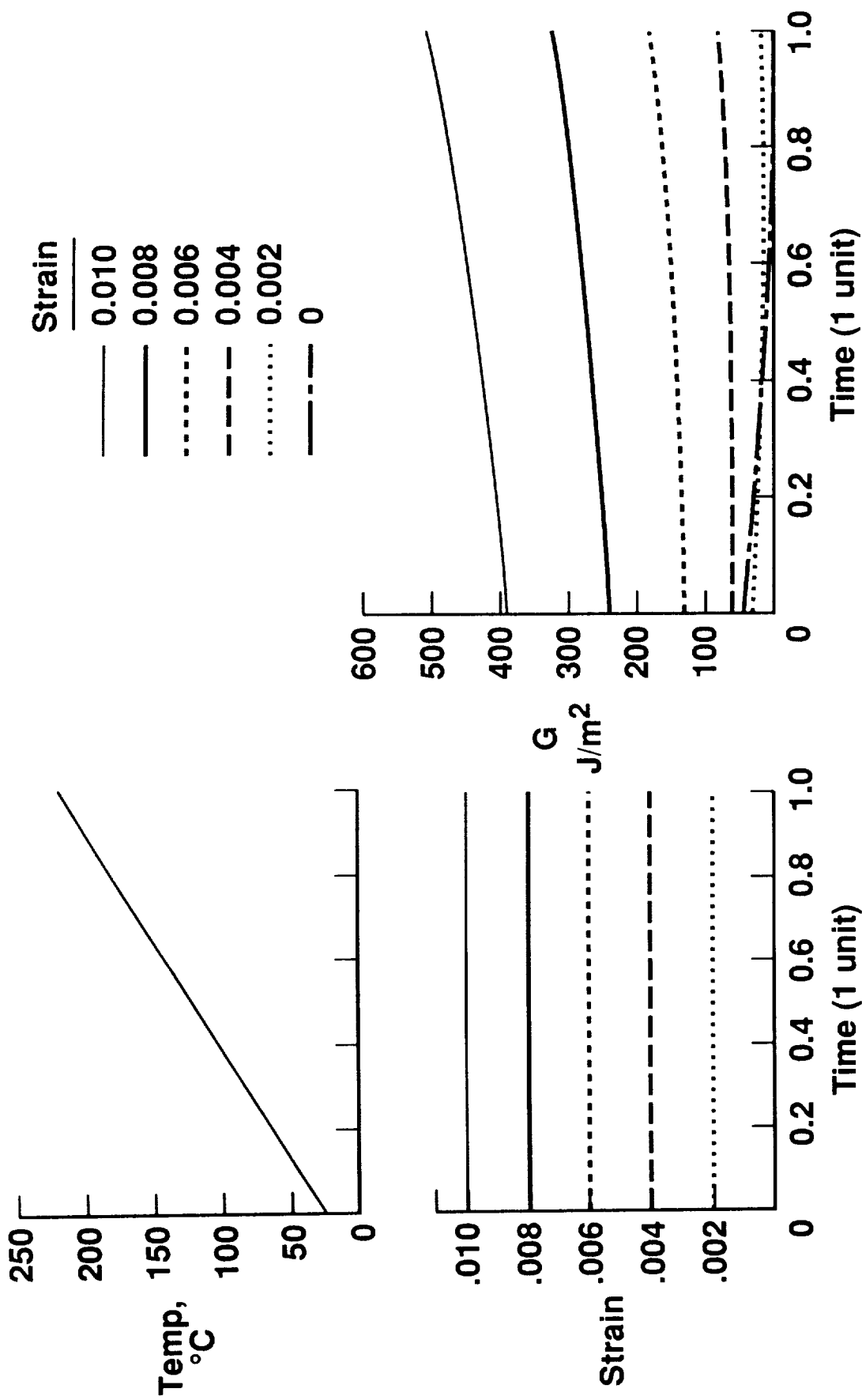
Fig. 6   G values at the edge of a [45/-45/0/90]ₛ laminate under
increasing temperature at various strains.
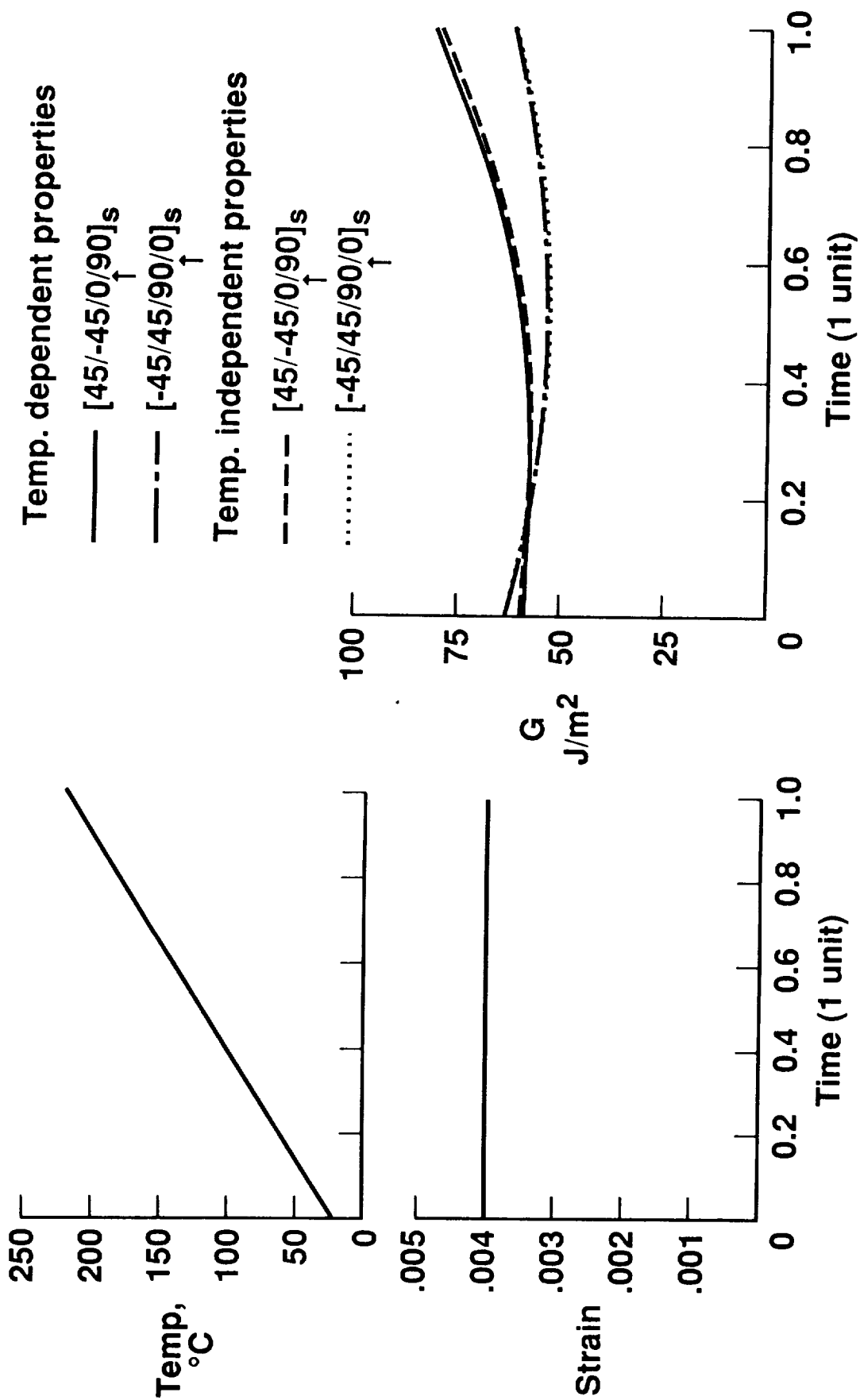
Fig. 7   G values at the edge of a [45/-45/0/90]$_s$ and a [-45/45/90/0]$_s$ laminate for temperature dependent and temperature independent materials.

[45/0/-45/90]s

[45/-45/0/90]s

[45/-45/90/0]s

[45/90/-45/0]s

G
J/m²

100

75

50

25

0

Time (1 unit)

0   0.2   0.4   0.6   0.8   1.0

Temp,
°C

200

150

100

50

0

Strain

.005

.004

.003

.002

.001

0

Time (1 unit)

0   0.2   0.4   0.6   0.8   1.0
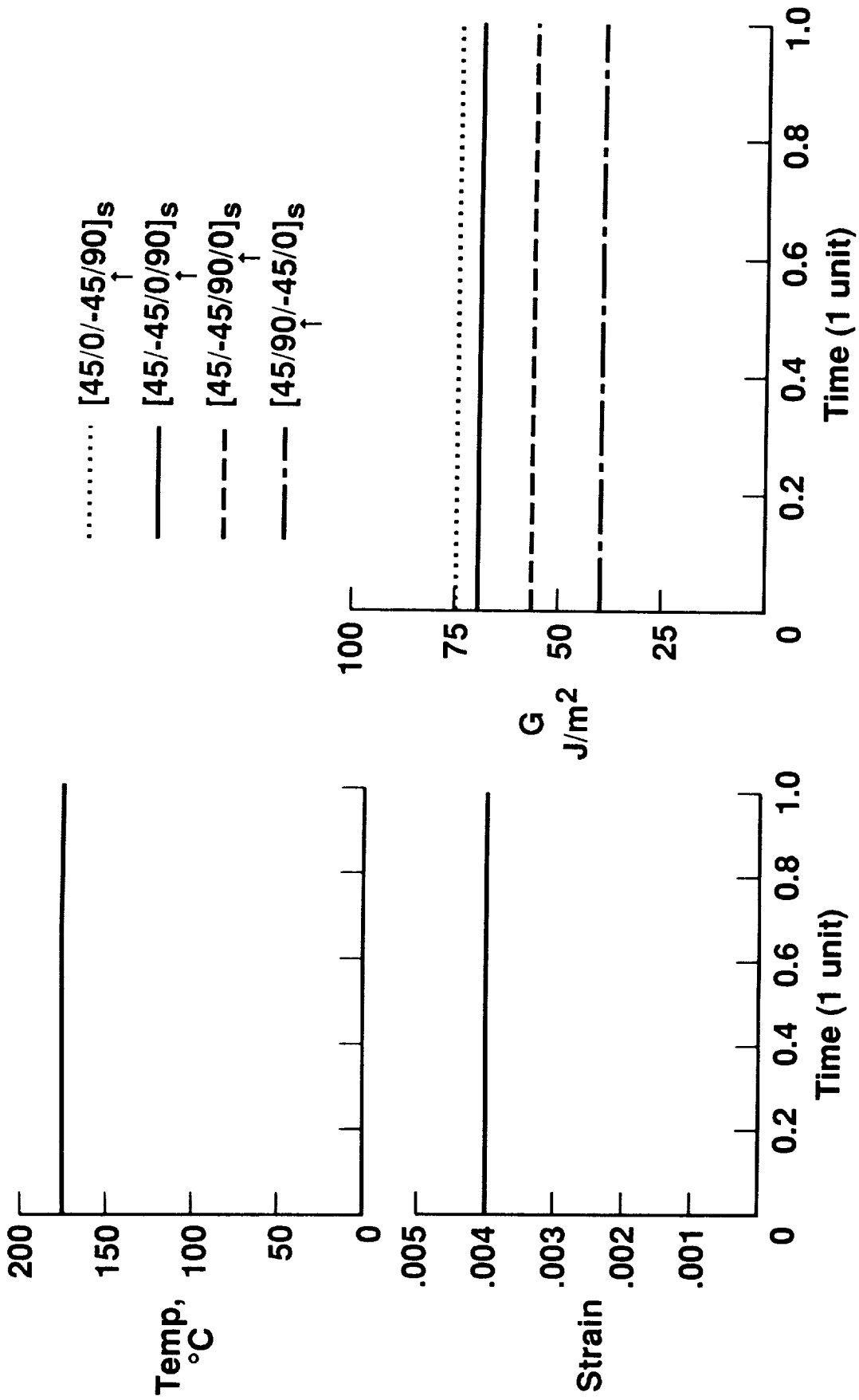
Fig. 8   G values at the edge for different quasi-isotropic lay-
ups.

38

E$_{22}$ decreasing from 1 to 0.5

E$_{22}$ decreasing from 1 to 0.5
and G$_{12}$ from 1 to 0.75

E$_{11}$ decreasing from 1 to 0.8
E$_{22}$ from 1 to 0.5 and G$_{12}$
from 1 to 0.75

G
J/m^2

[45/-45/0/90]$_s$

Temp,
°C

Strain

Time (1 unit)

Time (1 unit)
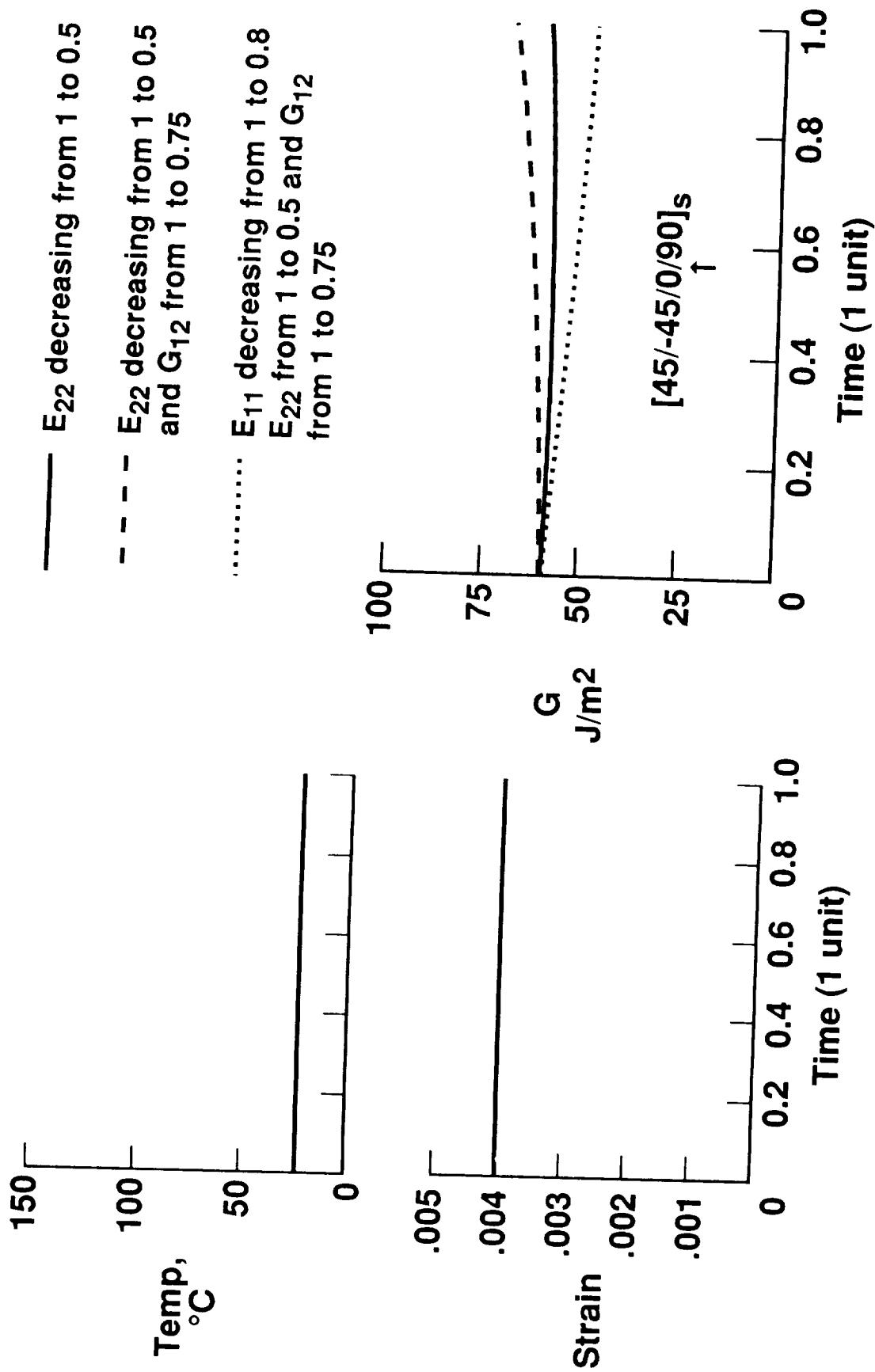
Fig. 9   G values at the edge of a [45/-45/0/90]$_s$ laminate with
properties varying with time.
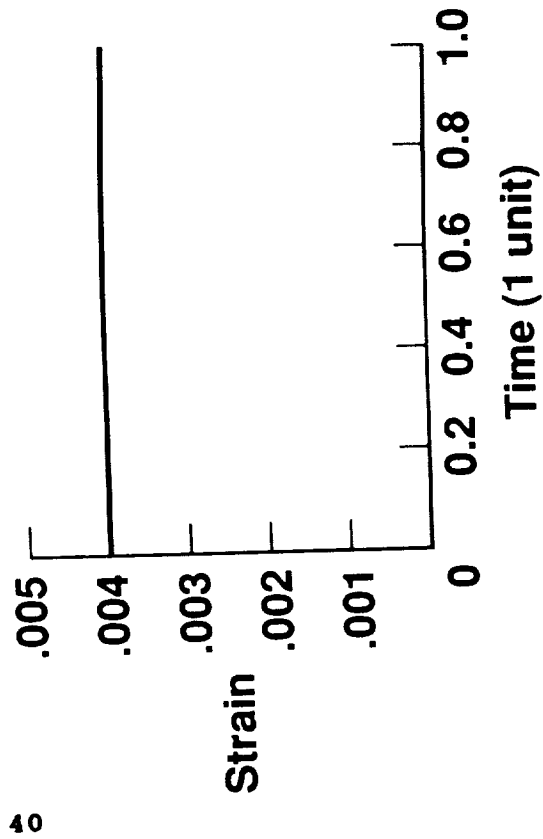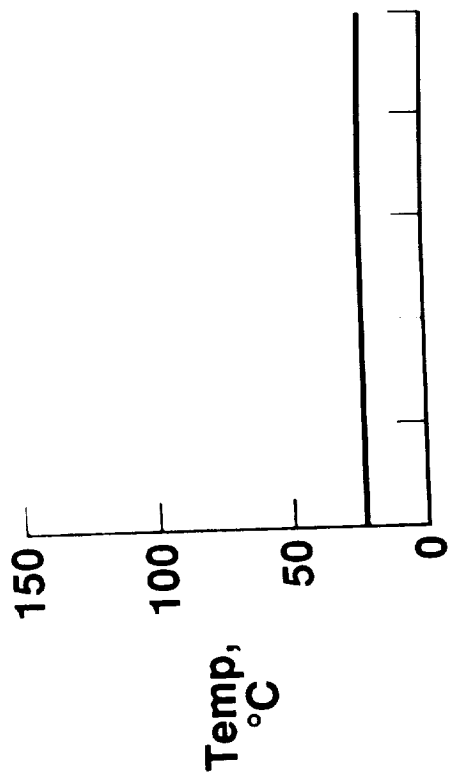
39

E22 decreasing from 1 to 0.5

E22 decreasing from 1 to 0.5
and G12 from 1 to 0.75

E11 decreasing from 1 to 0.8
E22 from 1 to 0.5 and G12
from 1 to 0.75

$[-45/45/90/0]_s$

G
J/m^2

Time (1 unit)

Temp,
°C

Strain

Time (1 unit)
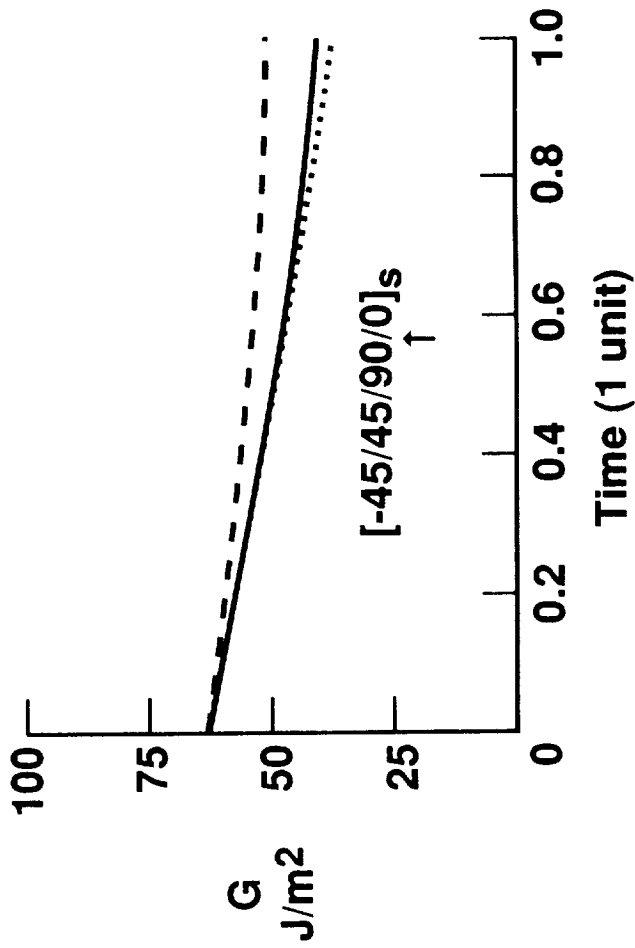
Fig. 10   G values at the edge of a $[-45/45/90/0]_s$ laminate with
properties varying with time.
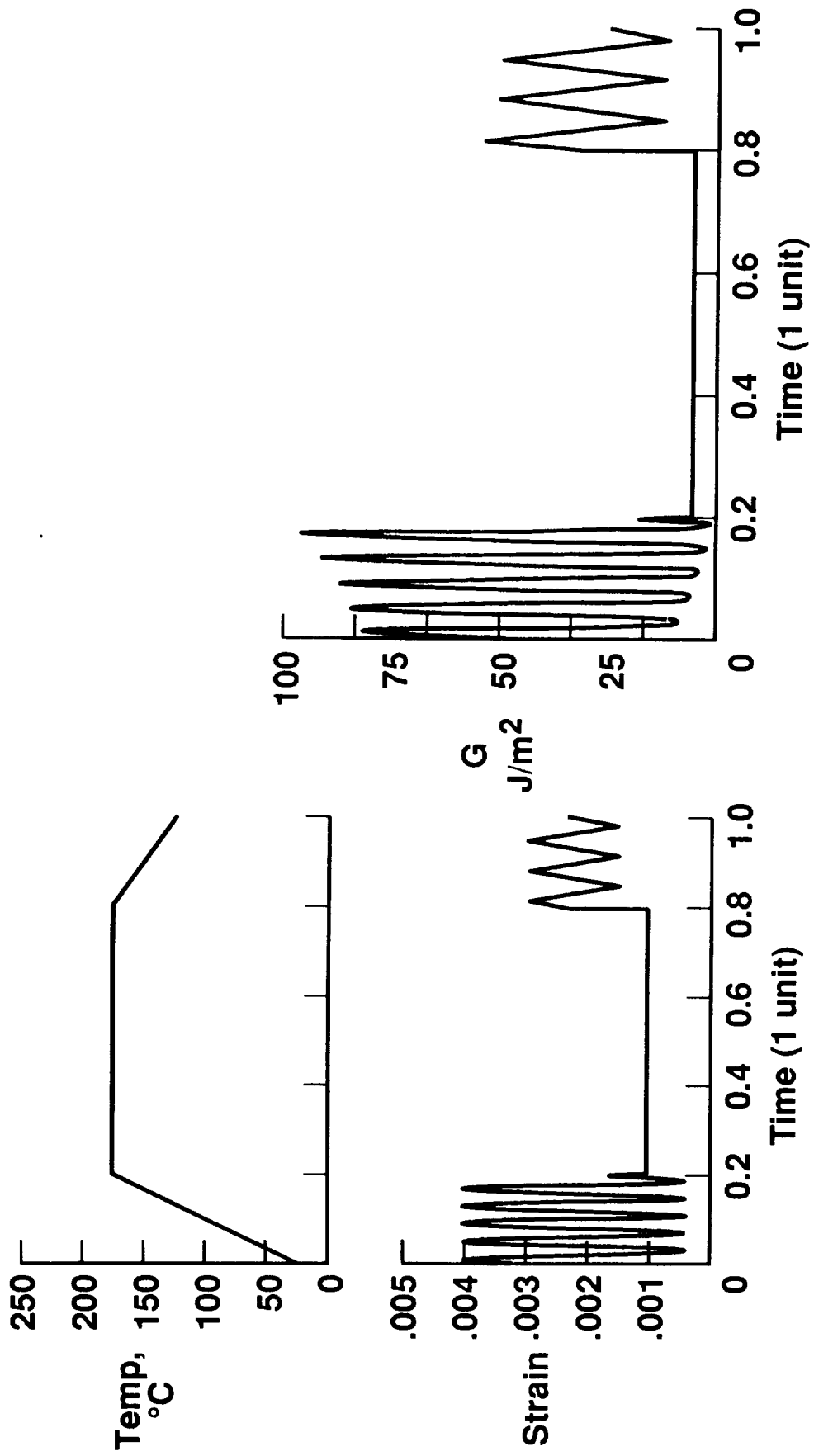
Fig. 11   G values at the edge of a $[45/-45/0/90]_s$ laminate under a simulated flight profile.
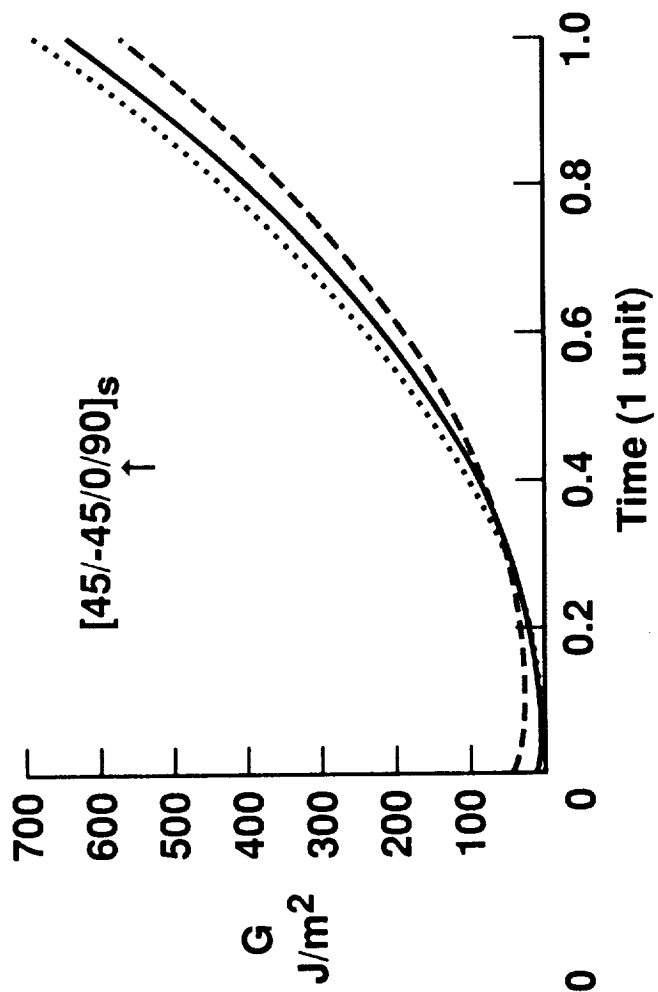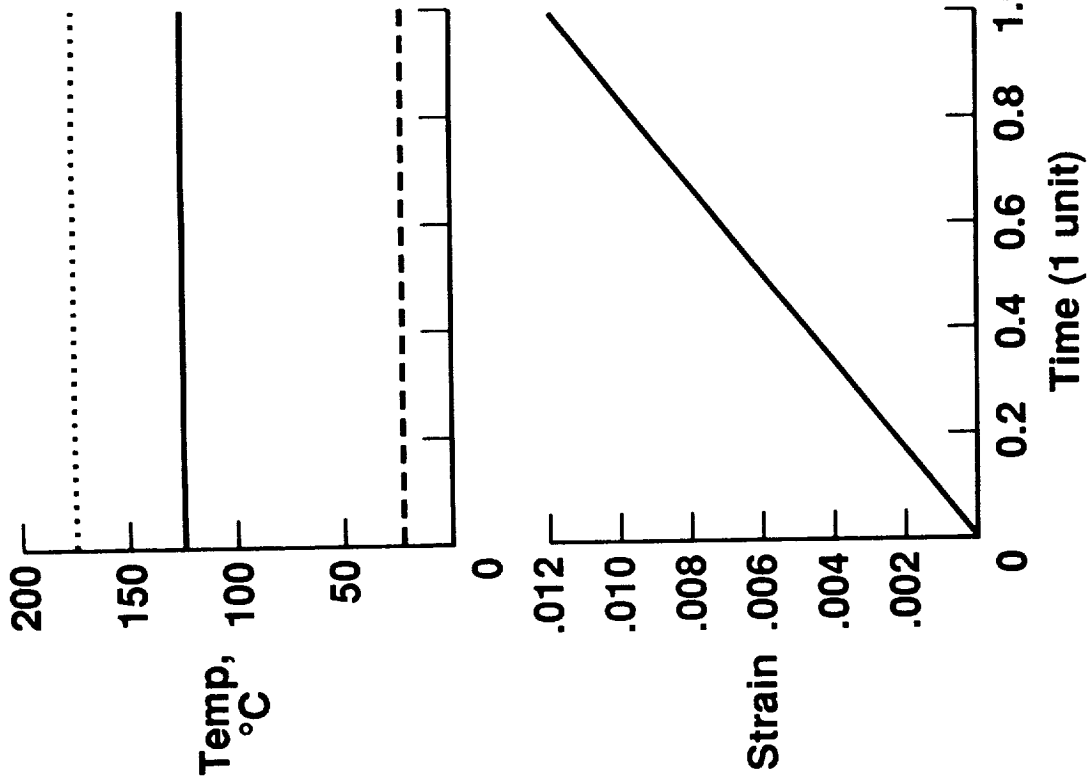
Fig. 12 G values at the edge of lay-up A under increasing strain at different temperatures.
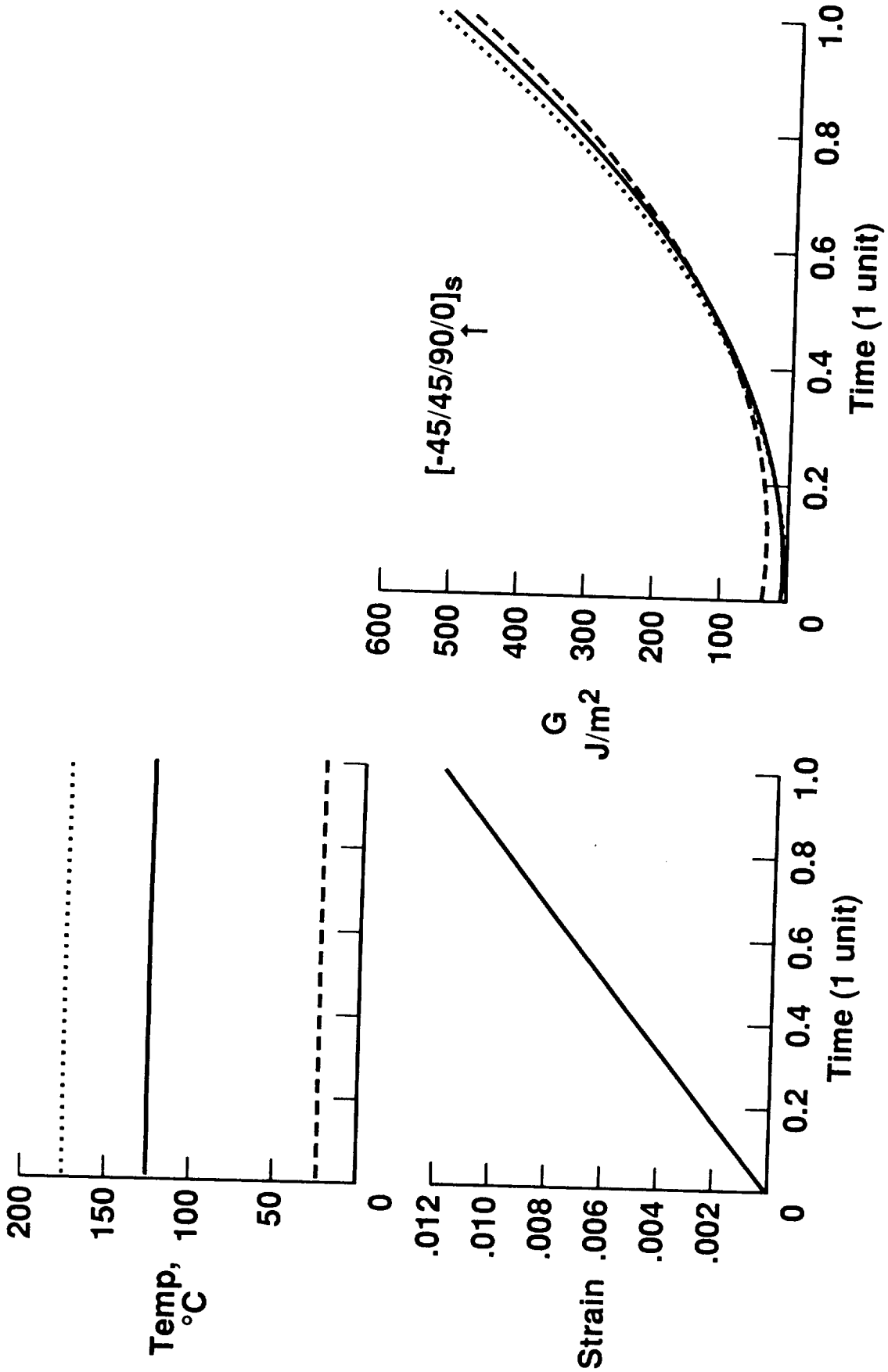
Fig. 13 G values at the edge of lay-up B under increasing strain at different temperatures.
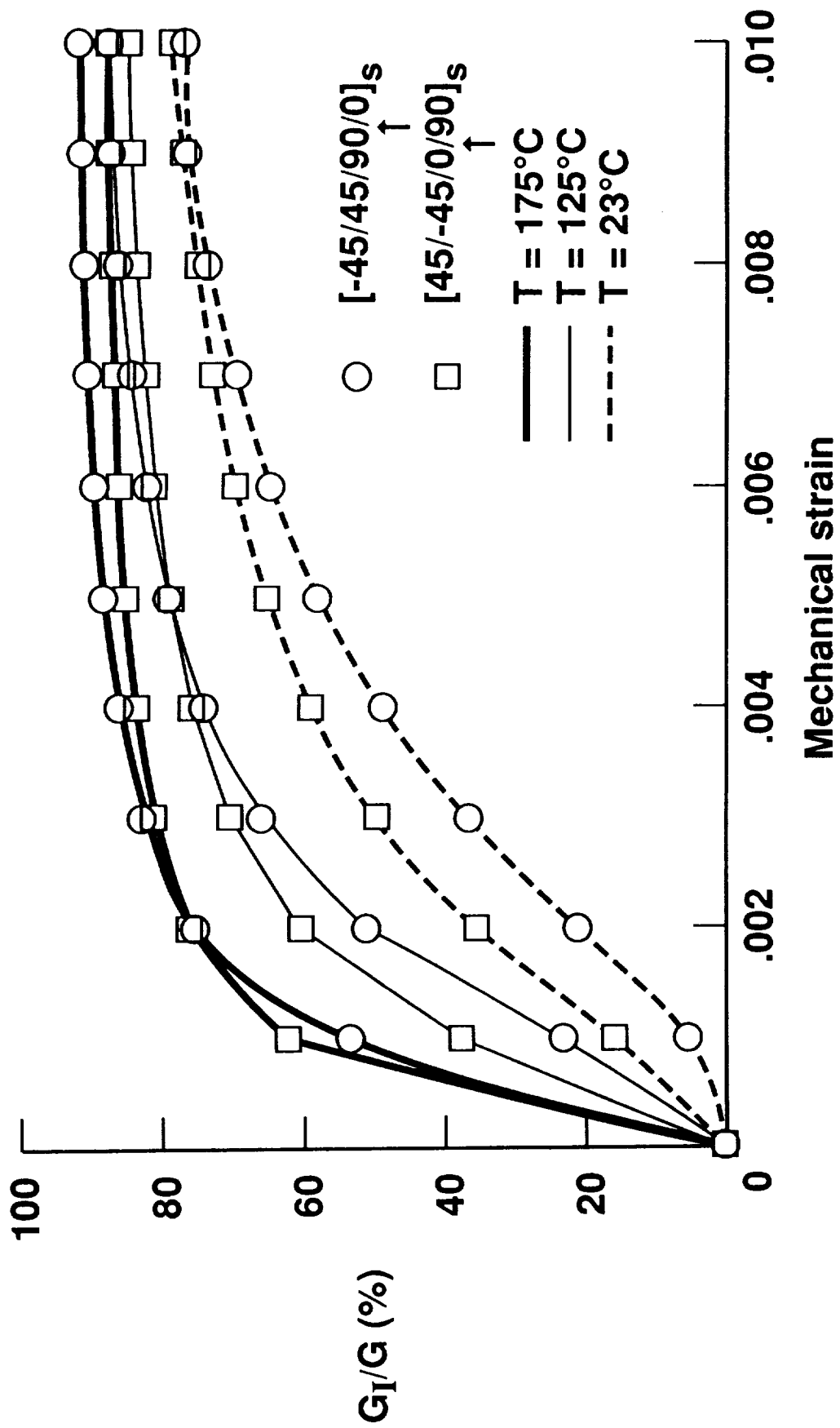
Fig. 14   Variation of G_I/G with increased strain at different temperatures.
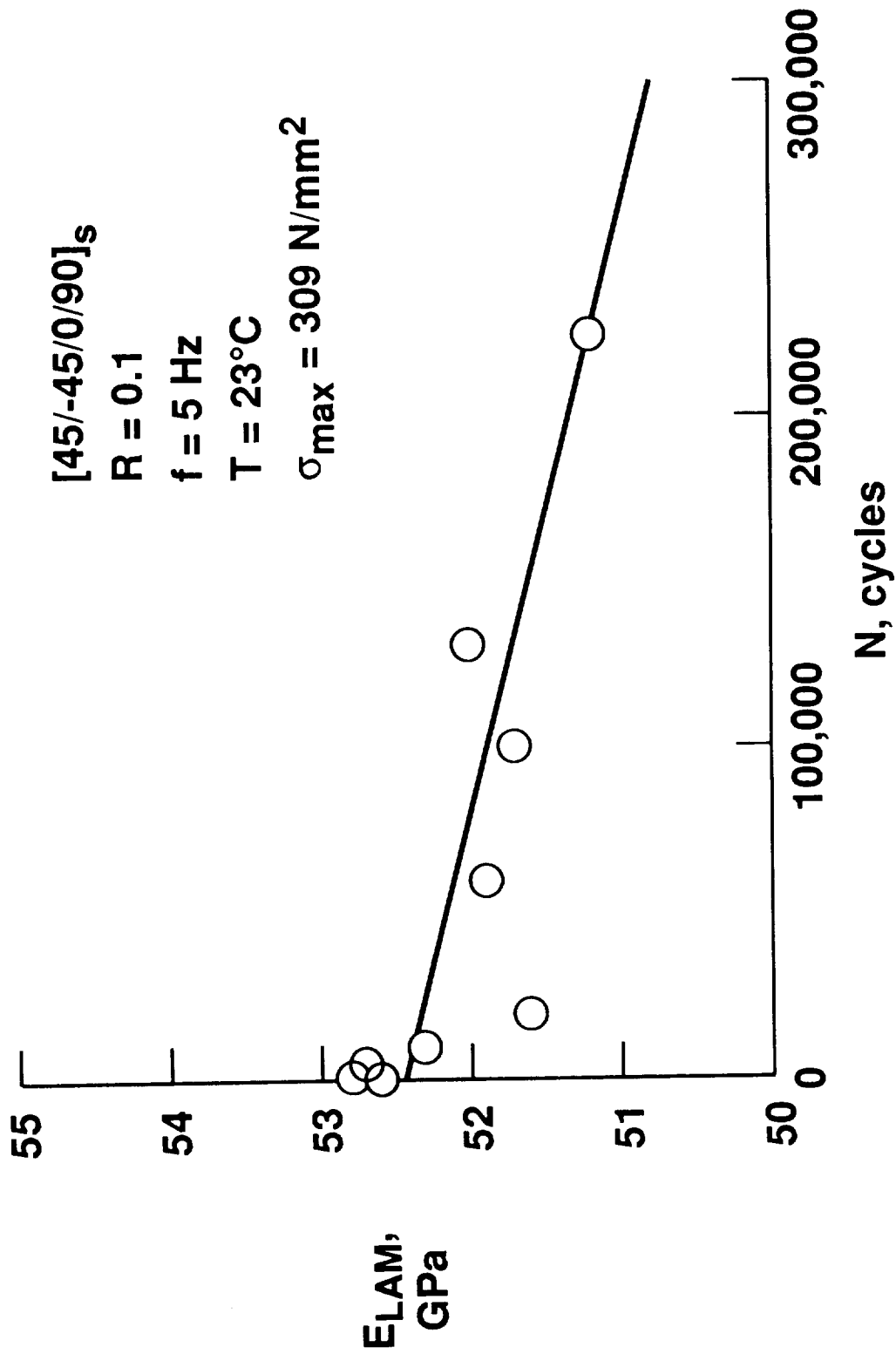
Fig. 15   Stiffness loss with cycles for lay-up A.

Fig. 16 Radiograph and micrograph of damage in lay-up A.
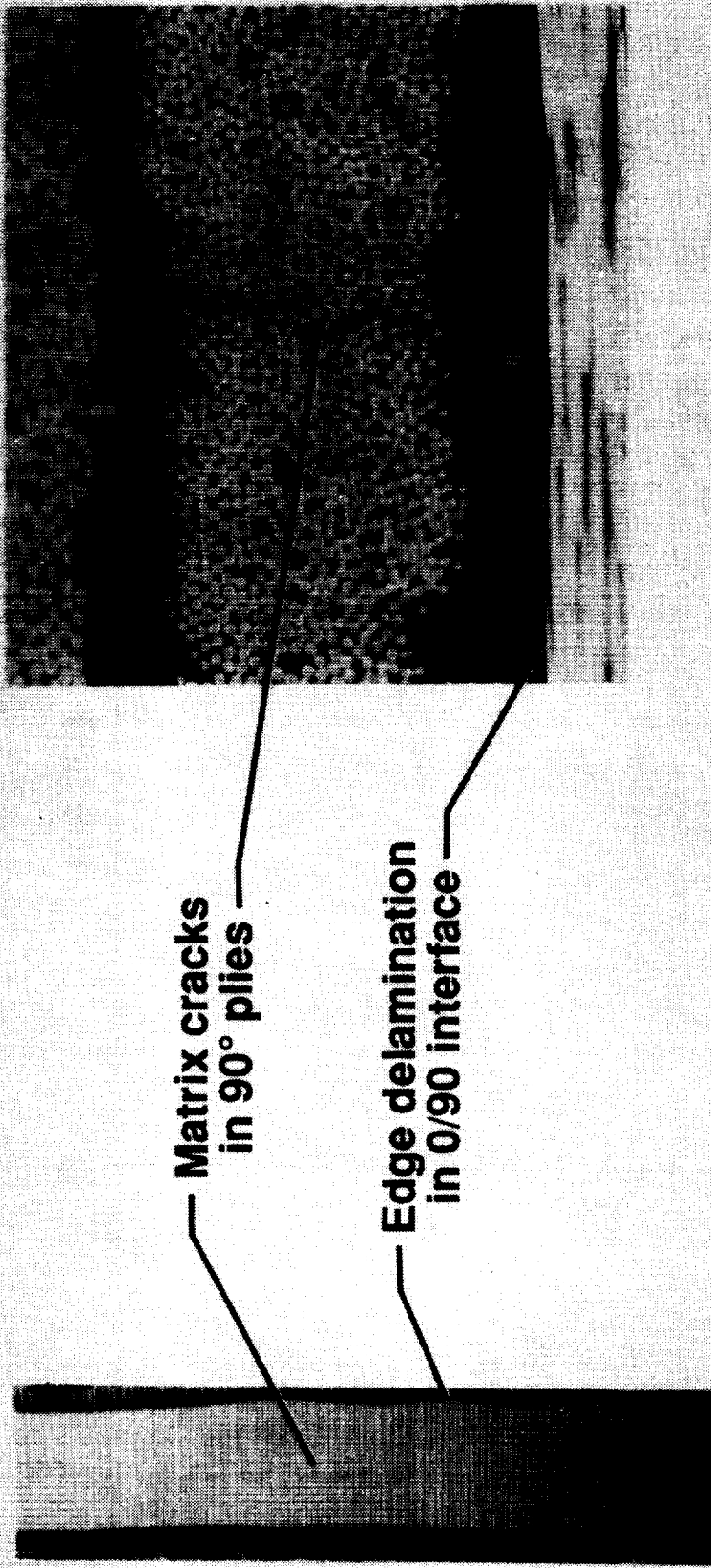
Matrix cracks in 90° plies

Edge delamination in 0/90 interface

46
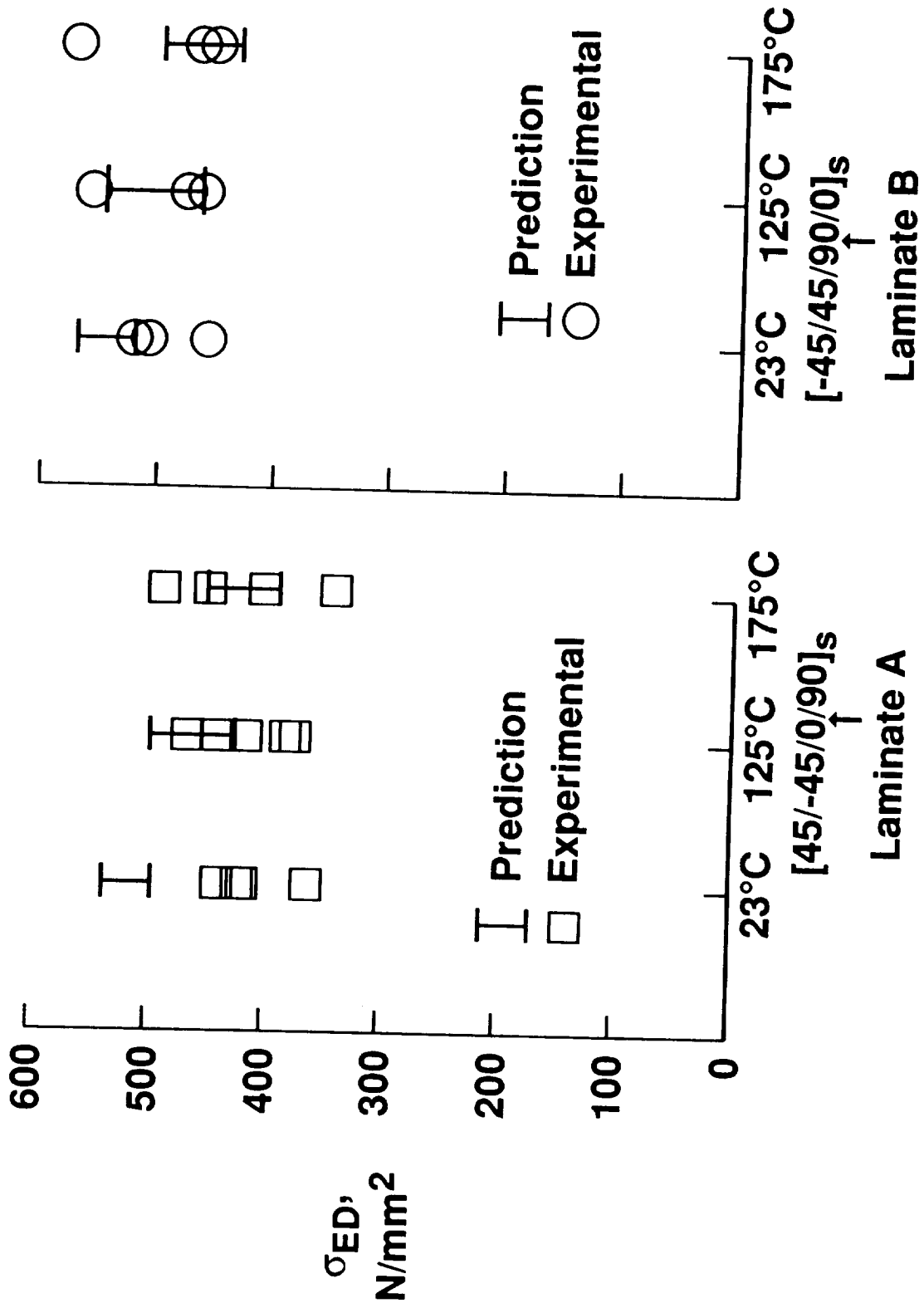
Fig. 17 Static test results and predictions for lay-ups A and B at isothermal temperatures.
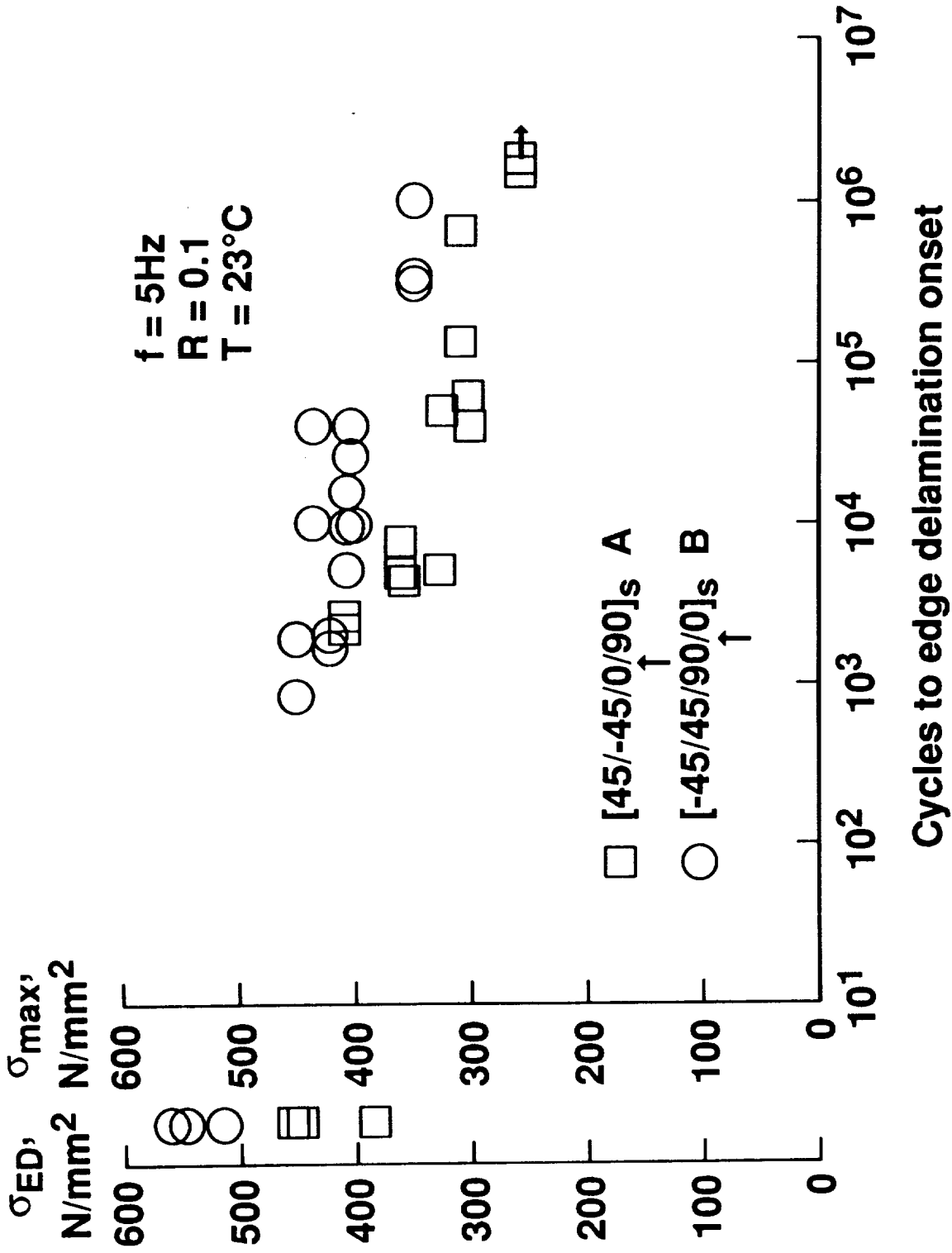
Fig. 18   Fatigue results for lay-up A and lay-up B at 23°C.
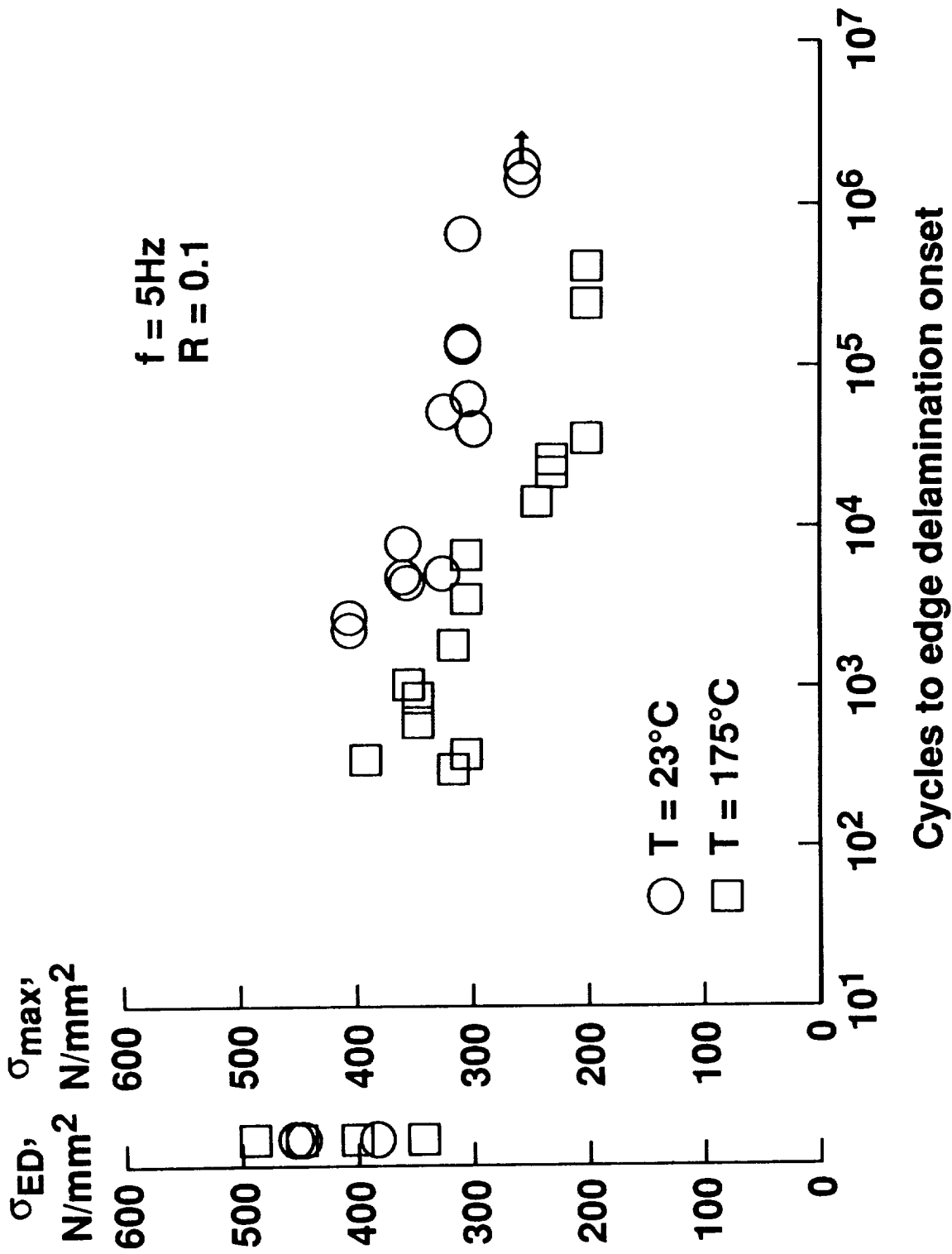
48
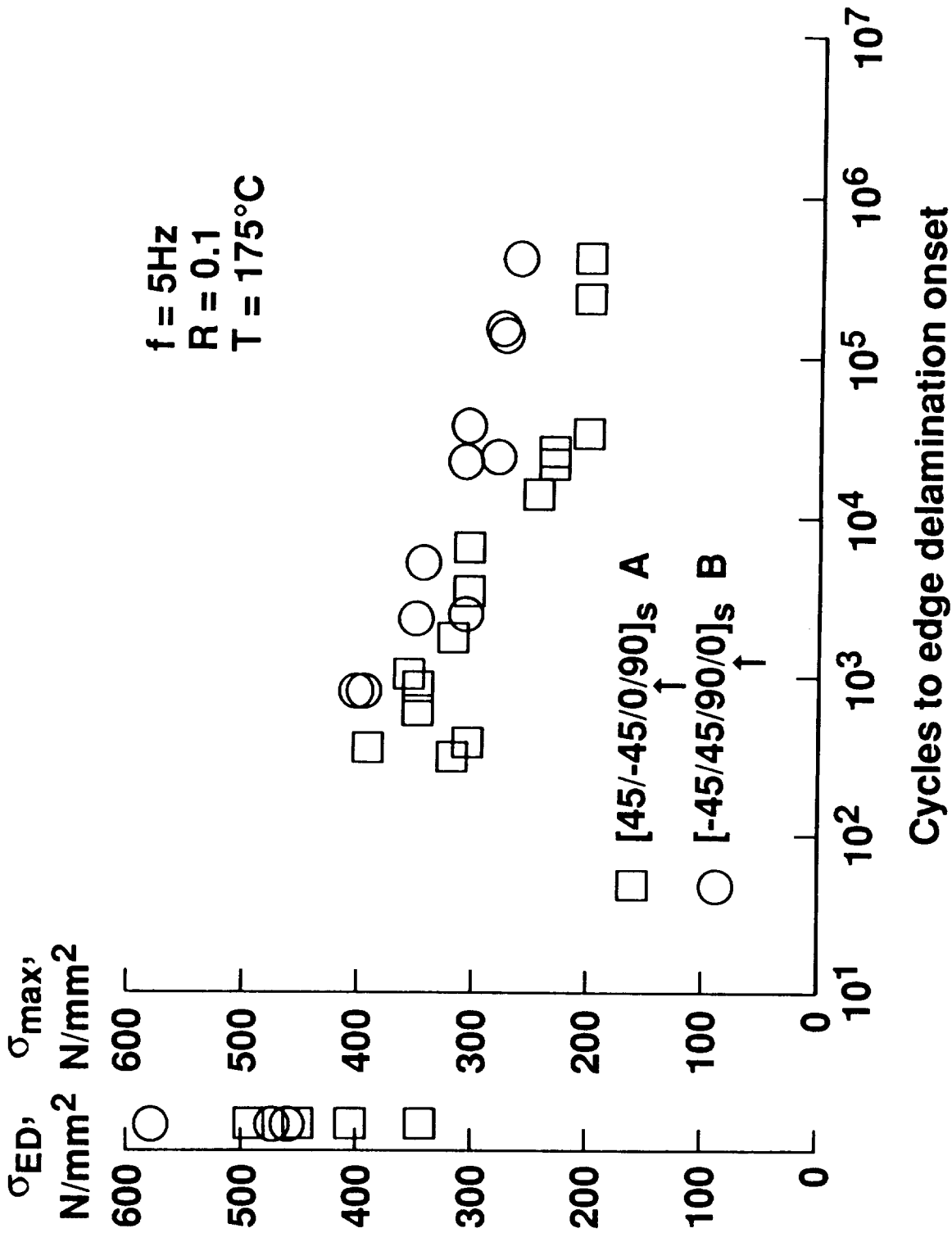
Fig. 19   Fatigue results for lay-up A and lay-up B at 175°C.
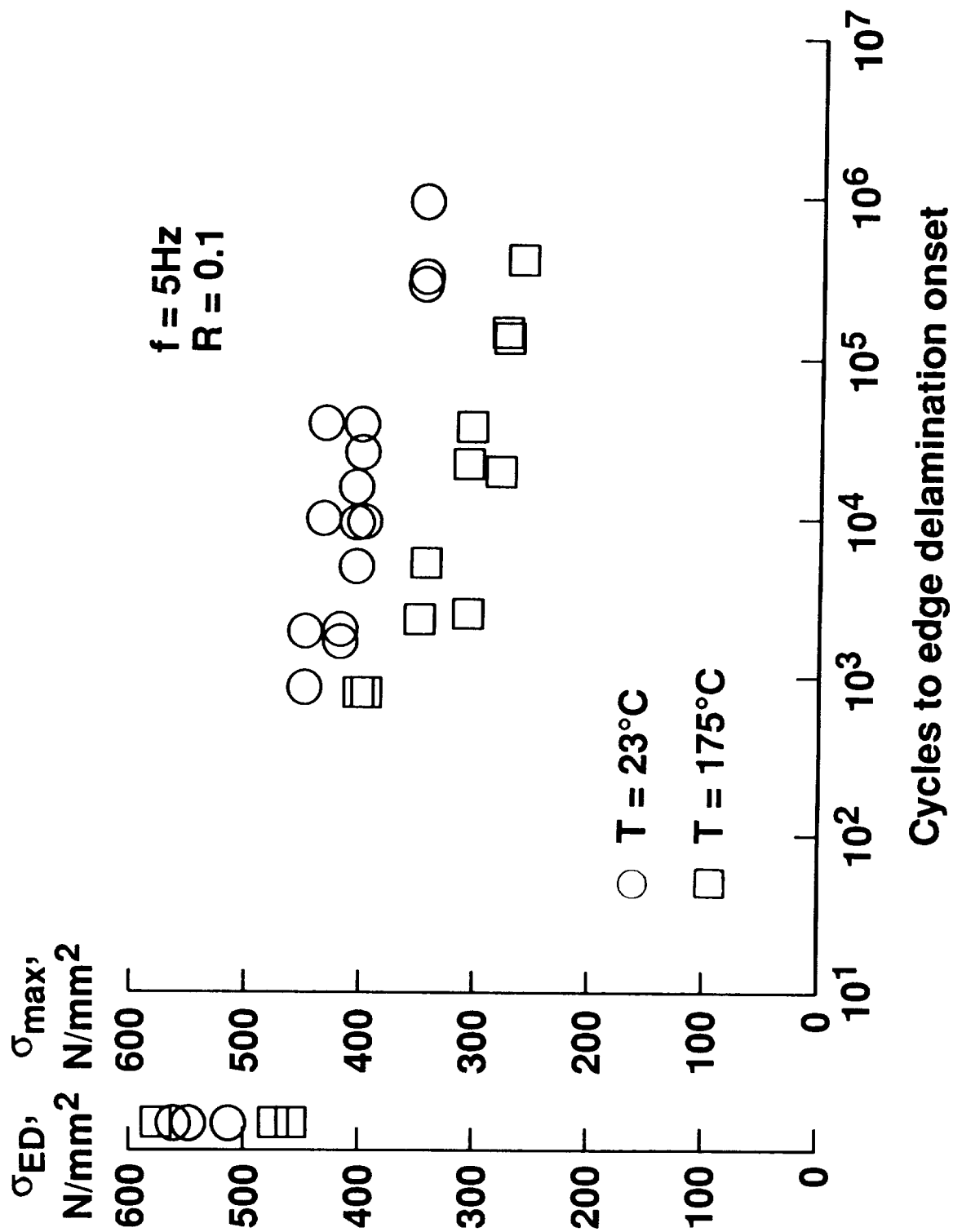
Fig. 20   Fatigue results for lay-up A at 23°C and 175°C.

50

Fig. 21   Fatigue results for lay-up B at 23°C and 175°C.
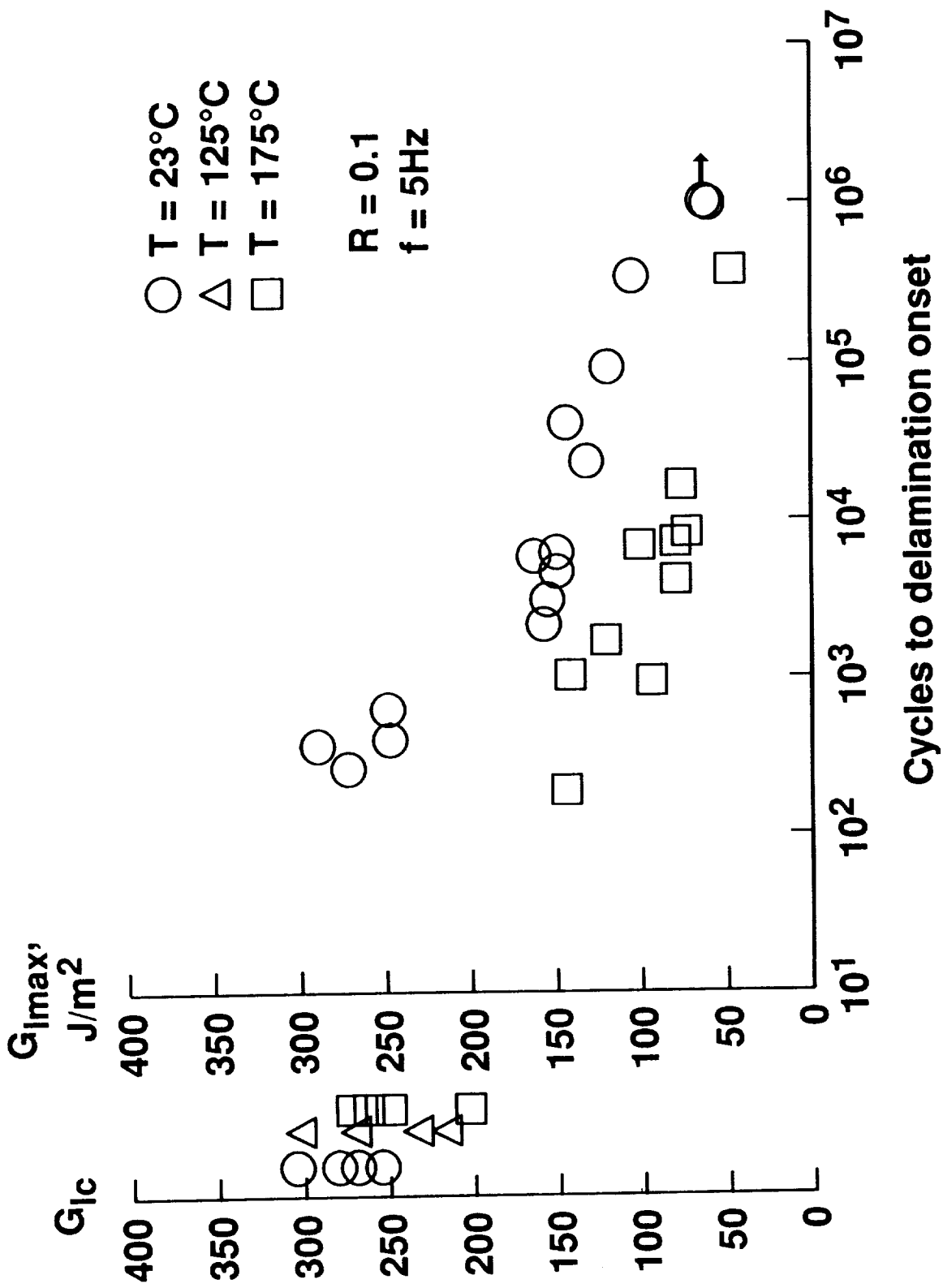
51

Fig. 22   G-N curve for DCB specimens at 23°C and 175°C.

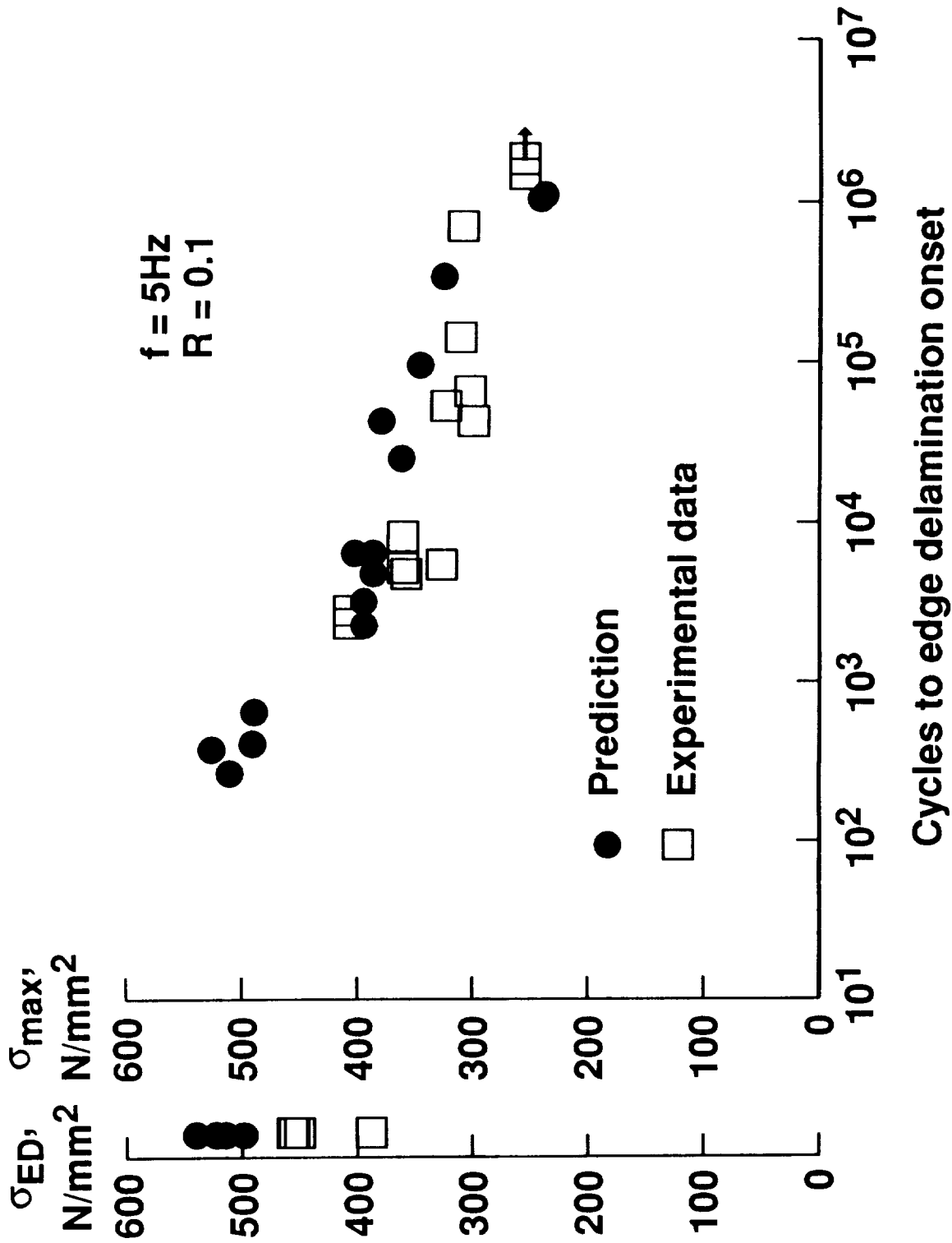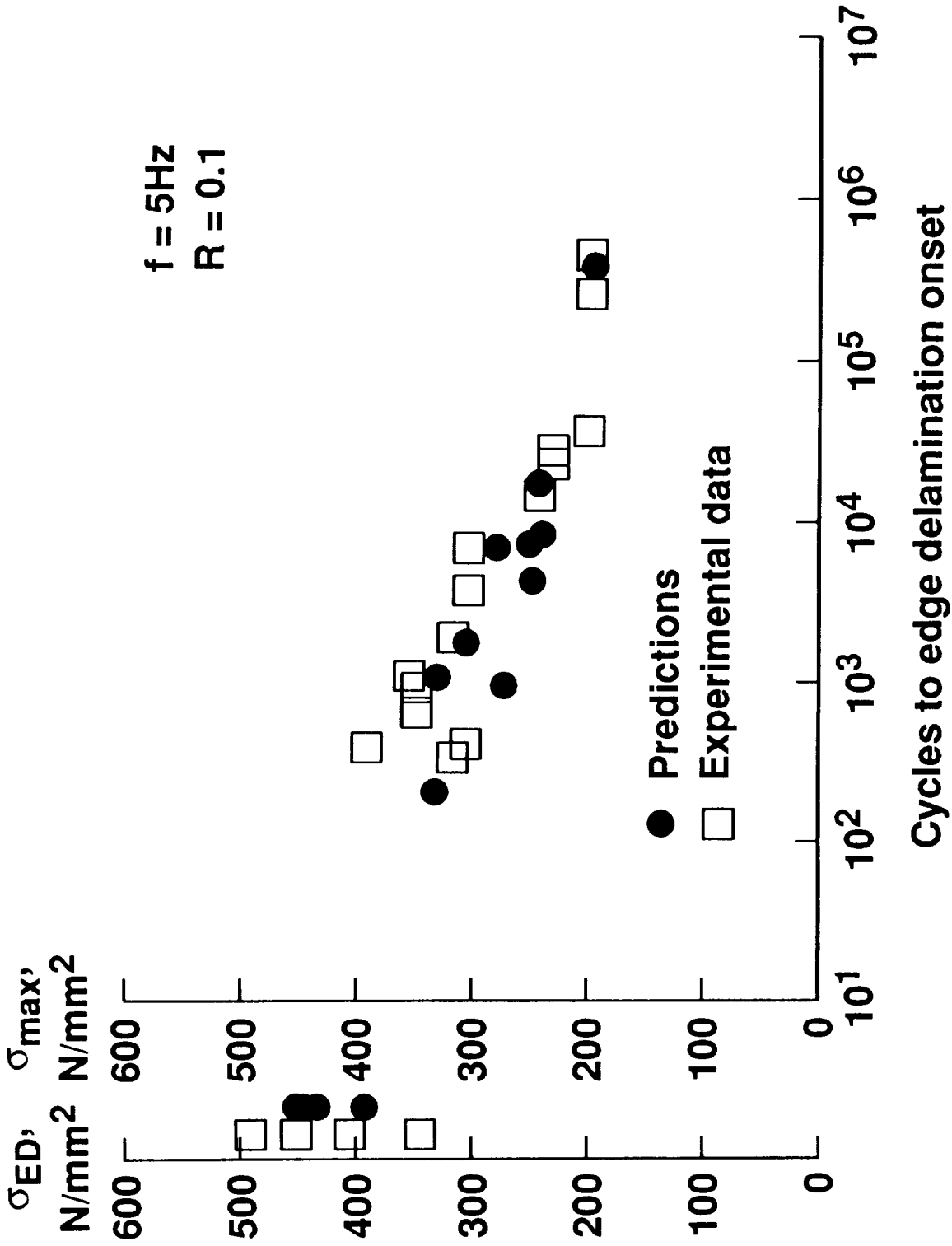Fig. 23 Fatigue predictions for lay-up A at 23°C.
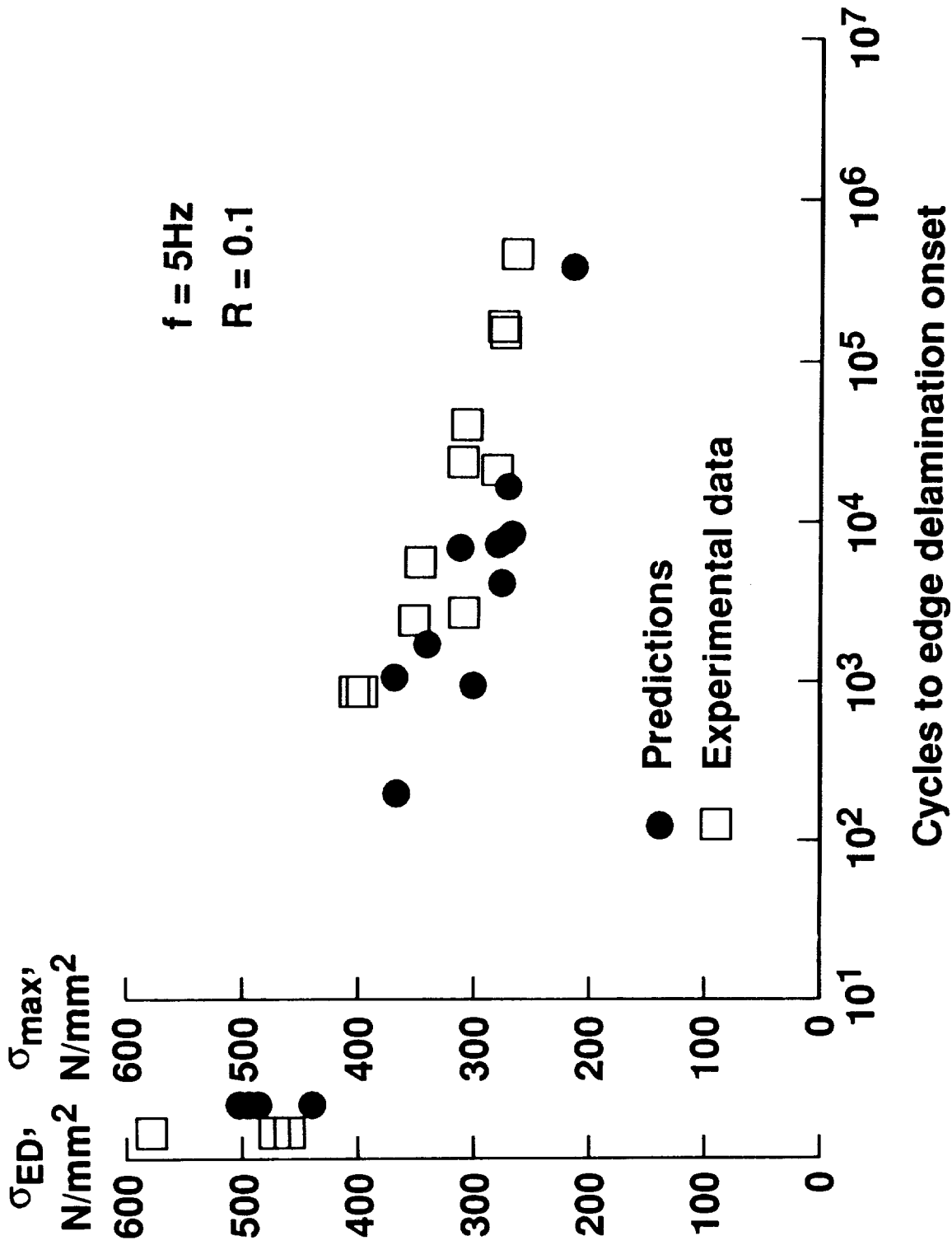
Fig. 24   Fatigue predictions for lay-up B at 23°C.

Fig. 25 Fatigue predictions for lay-up A at 175°C.

Fig. 26   Fatigue predictions for lay-up B at 175°C.

REPORT DOCUMENTATION PAGE

Public reporting burden for this collection of information is estimated to average 1 hour per response, including the time for reviewing instructions, searching existing data sources, gathering and maintaining the data needed, and completing and reviewing the collection of information. Send comments regarding this burden estimate or any other aspect of this collection of information, including suggestions for reducing this burden, to Washington Headquarters Services, Directorate for Information Operations and Reports, 1215 Jefferson Davis Highway, Suite 1204, Arlington, VA 22202-4302, and to the Office of Management and Budget, Paperwork Reduction Project (0704-0188), Washington, DC 20503.

1. AGENCY USE ONLY (Leave blank)	2. REPORT DATE November 1991	3. REPORT TYPE AND DATES COVERED Contractor Report

4. TITLE AND SUBTITLE
Delamination Onset in Polymeric Composite Laminates Under Thermal and Mechanical Loads

5. FUNDING NUMBERS
NAS1-19399
505-63-50-04

6. AUTHOR(S)
Roderick H. Martin

7. PERFORMING ORGANIZATION NAME(S) AND ADDRESS(ES)
Analytical Services and Materials, Inc.
107 Research Drive
Hampton, VA 23666

8. PERFORMING ORGANIZATION REPORT NUMBER

9. SPONSORING/MONITORING AGENCY NAME(S) AND ADDRESS(ES)
National Aeronautics and Space Administration
Langley Research Center
Hampton, VA 23665-5225

10. SPONSORING/MONITORING AGENCY REPORT NUMBER
NASA CR-189548

11. SUPPLEMENTARY NOTES
Langley Technical Monitor: Charles E. Harris
Paper presented at the ASTM Symposium on High Temperature and Environmental Effects on Polymeric Composites; San Diego, CA; October 15, 1991.

12a. DISTRIBUTION/AVAILABILITY STATEMENT

Unclassified - Unlimited

Subject Category - 39

12b. DISTRIBUTION CODE

13. ABSTRACT (Maximum 200 words)

This paper describes a fracture mechanics damage methodology to predict edge delamination. The methodology accounts for residual thermal stresses, cyclic thermal stresses and cyclic mechanical stresses. The modeling is based on the classical lamination theory and a sublaminate theory. The prediction methodology determines the strain energy release rate, G, at the edge of a laminate and compares it with the fatigue and fracture toughness of the composite. To verify the methodology, isothermal static tests at 23°C, 125°C, and 175°C and tension-tension fatigue tests at 23°C and 175°C were conducted on laminates. The material system used was a carbon/bismaleimide, IM7/5260. Two quasi-isotropic layups were used, [45/-45/0/90]s and [-45/45/90/0]s. Also, 24-ply unidirectional double cantilever beam specimens were tested to determine the fatigue and fracture toughness of the composite at different temperatures. Raising the temperature had the effect of increasing the value of G at the edge for these layups and also to lower the fatigue and fracture toughness of the composite. Exprimentally, the static stress to edge delamination was not effected by temperature but the number of cycles to edge delamination decreased. The ply interface for delamination was well predicted as was the number of cycles to edge delamination. The static stress predictions tended to overestimate the actual test results, particularly at room temperature.

14. SUBJECT TERMS
Strain energy release rate; Interlaminar fracture toughness; Isothermal fatigue; Double cantilever beam; Supersonic transport

15. NUMBER OF PAGES
57

16. PRICE CODE
A04

17. SECURITY CLASSIFICATION OF REPORT Unclassified	18. SECURITY CLASSIFICATION OF THIS PAGE Unclassified	19. SECURITY CLASSIFICATION OF ABSTRACT	20. LIMITATION OF ABSTRACT